Fire Safety Journal 158 (2025) 104545

Contents lists available at ScienceDirect

Fire Safety Journal

journal homepage: www.elsevier.com/locate/firesaf

Thresholds of surface fire transition to crown fire: Effects of wind speed and crown base height with fixed moisture content

Mohamed Sharaf [a,d,*], Duncan Sutherland [b], Rahul Wadhwani [a,c], Khalid Moinuddin [a]

[a] Institute of Sustainable Industries and Liveable Cities, Victoria University, Melbourne, Australia
[b] School of Science, University of New South Wales, Canberra, Australia
[c] Human Dimension, Rocky Mountain Research Station, United States Department of Agriculture, Missoula, MT, USA
[d] Mechanical Engineering Department, Benha Faculty of Engineering, Benha University, Benha, Egypt

ARTICLE INFO

Keywords:
Fire dynamic simulator (FDS)
Wind speed
Crown base height (CBH)
Pine forest
Fire transition
Surface fire
Crown fire

ABSTRACT

Forest fires present significant global risks, leading to loss of life, community displacement, and extensive damage to property and the environment, with substantial economic and social consequences. Propagation of wildland fires can be divided into two categories: surface and crown fires. This study aims to identify threshold parameters that influence the transition from surface to crown fire, helping fire managers prevent manageable fires from escalating into uncontrollable crown fires. This study conducted pine forest simulations using the physics-based fire model Fire Dynamics Simulator (FDS) to examine the effects of varying wind speeds and crown base heights on fire transition. The results identify that 80 % crown mass loss represents sustained crowning, while values between 65 % and 80 % correspond to intermediate crowning. Furthermore, the findings demonstrate that wind speed and crown base height are crucial in reaching these threshold values. A reduction in crown base height substantially increases the likelihood of sustained crowning. However, the influence of wind speed on the surface fire transition varies with crown base height. These findings enhance understanding of surface fire transition and offer valuable insights for forest fire management and prevention.

1. Introduction

Surface fires play a significant role in how fires spread by moving across the ground-level fuels [1]. Surface fires can intensify, scorching or destroying forest canopies by igniting lower branches, particularly in dry, windy conditions. This leads to fast, intense crown fires, marked by towering flames (30–60 m), rapid spread (10–15 km/h), and firebrands that ignite new fires ahead. The immense energy release, combined with strong winds and plume entrainment, makes crown fires highly destructive [2].

Van Wagner [3] classified crown fires into passive, active, and independent. In a passive crown fire, the crown fuels do not form a continuous fire line and may burn only partially, with the overall fire behaviour primarily influenced by the surface fire. In an active crown fire, the crown fuels burn continuously as a fire line, and the fire behaviour is dictated mainly by the propagation across the crown. Independent crown fires spread exclusively across the crown fuels while not affecting the surface fuels [4]; they are rare and occur for short periods and under extreme wind and/or steep slopes. The transition from surface to crown fires depends on several key factors, including surface fire intensity, crown base height (CBH), wind speed, and fuel properties [5] (e.g., fuel moisture content, canopy density). Understanding these factors is essential for predicting and managing crown fires. However, the interplay between these variables is complex, making it challenging to develop accurate predictive models.

The transition from surface to crown fires is governed by several physical processes, including heat transfer (both radiative and convective), flame dynamics, and fuel ignition. When a surface fire burns, it releases energy that heats the surrounding air and fuels. If the surface fire intensity is sufficiently high, the heat can ignite the lower branches of the canopy, leading to a crown fire. The crown base height plays a crucial role in the fire transition, as lower heights increase the proximity of the canopy to the surface fire, facilitating vertical fire spread through flames, radiant heat, and embers [6]. Wind speed also significantly influences the transition. Higher winds enhance convective heat transfer, accelerating surface fire spread and increasing the likelihood of igniting lower branches, thereby aiding crown fire transition [7]. However, extremely high winds (over 100 km/h) can reduce flame residence time,

* Corresponding author. Institute of Sustainable Industries and Liveable Cities, Victoria University, Melbourne, Australia.
E-mail addresses: Mohamed.sharaf@live.vu.edu.au, Mohamed.sharaf@bhit.bu.edu.eg (M. Sharaf).

https://doi.org/10.1016/j.firesaf.2025.104545
Received 3 May 2025; Received in revised form 18 August 2025; Accepted 18 September 2025
Available online 22 September 2025

preventing crown fire initiation [8]. In contrast, low wind conditions allow plume-driven vertical movement to dominate, enabling upward spread within the canopy, especially when crown fuels are dry [9]. One study that has explored the effects of wind and ignition conditions on forest crown fire dynamics is that of Grinshin and Perminov [10], who used numerical analysis to study the transition from surface to crown fire in young pine wood, focusing on temperature and pyrolysis gas distribution under different ignition conditions. They found that wind does not affect the transition in young pine wood, with ignition requiring a minimum pulse (energy per unit area) of 4000 kJ/m^2, which means the total amount of energy required to ignite the tree crowns from the forest ground fire. Additionally, they identified the critical height between the surface and the crown to be 0.5 m.

Over the past few decades, several models have been developed to predict crown fire initiation and spread. Van Wagner [3] proposed a semi-empirical model that identifies the critical surface fire intensity $I_{critical\_vw}$ (KW/m) required for crown fire initiation, expressed as:

$$I_{critical\_vw} = (C(CBH)h)^{\frac{3}{2}} \tag{1}$$

where CBH represents the crown base height, h denotes the heat of ignition (kJ/kg) for crown ignition, and C is a constant in the empirical model. This model highlights the importance of surface fire intensity and crown base height in determining the transition to crown fire.

Building on Van Wagner's work, Scott [11] developed a formula for the critical fire line intensity $I_{critical\_Scott}$ needed for surface fire to transition to crown fire, incorporating crown moisture content:

$$I_{critical\_Scott} = \left[\frac{CBH\,(460 + 25.9\,FMC\,)}{100} \right]^{1.5} \tag{2}$$

Here, FMC (%) is crown moisture content. These models have been widely used in operational fire management, but they rely on empirical data and may not capture the full complexity of fire behaviour under varying conditions.

Cruz et al. [12–19] and Alexander and Cruz [20] developed multiple models for predicting crown fire initiation and spread using experimental datasets from North American conifer forests. These models identified key influencing parameters, such as wind speed, canopy bulk density, and surface fuel consumption. While these models have proven useful for operational fire prediction, their reliance on specific datasets limits their applicability to broader geographic regions with different forest compositions and thermo-physical properties. Additionally, these models often assume homogenous fuel conditions, which may not reflect the variability found in real-world fire scenarios.

While empirical models offer rapid predictions, they are limited by their reliance on outdated data and may yield non-physical results, especially in regions with sparse fire behavior data [21]. Physics-based models, such as the Fire Dynamics Simulator (FDS) developed by NIST, overcome these limitations by simulating fire behaviour using principles of physics and chemistry. FDS models complex processes like pyrolysis, combustion, turbulence, and heat transfer, delivering a dynamic, three-dimensional (3D) view of fire spread across diverse scenarios, including building fires and vegetative fuels. Its extension, the Wildland Urban Interface Fire Dynamics Simulator (WFDS), developed with the U. S. Forest Service, incorporates vegetation-specific fuel models (e.g., linear and Arrhenius thermal degradation sub-models) to simulate fire in wildland-urban interface zones [22,23]. Validated for scenarios like grassland surface fires, FDS, paired with its visualization tool Smoke View, is widely used to predict fire progression, smoke movement, and suppression effects [24].

Castle et al. [25] undertook a laboratory-scale investigation to comprehend the factors responsible for the transition from surface to crown fires. The primary focus was to assess the efficacy of the (WFDS) v4 in simulating this critical transition. Various scenarios were examined, encompassing diverse crown fuel densities and varying wind speeds. The simulations using WFDS-V4 showed results that aligned with trends observed in laboratory experiments. It was observed that higher crown fuel bulk densities significantly reduced the crown fuel's ignition success, a consistent finding across both the experimental and numerical outcomes. Furthermore, escalating wind velocities played a crucial role in increasing the consumption of the crown vegetation. Moinuddin and Sutherland [26] examined the ability of WFDS v6 to simulate the fire transition from surface to crown fire. WFDS v6 is more advanced, incorporating updates and bug fixes, and aligns more closely with the features of FDS v6; it expands the range of vegetation types and fuel modelling capabilities, with improved accuracy in simulating fire spread and interaction with vegetative fuels [27]. WFDS v6 offers better stability, improved algorithms, and enhanced fire dynamics for built and vegetated environments. Moinuddin and Sutherland [26] showed that the surface fire's propagation rate closely matches the crown fire's, indicating surface fire support. Once established, the crown fire achieves a quasi-steady heat release rate HRR. However, these simulations used fixed parameters, leaving potential variations from changes in thermo-physical, wind, and combustion parameters unexplored.

In recent studies, FDS has been validated for its ability to simulate complex fire behaviours. For example, Mueller et al. [22] used FDS 6.7.9 to investigate flame spread in pine needle beds, incorporating simple thermal decomposition models and improved char oxidation mechanisms. Their work demonstrated that using species-specific parameters enhanced the accuracy of mass loss rate MLR predictions, bringing simulated results within experimental uncertainty. Similarly, Wadhwani et al. [23] employed FDS 6.7.8 to simulate interactions between parallel merging surface fires, achieving relative errors of 5–35 % in the rate of fire spread compared to experimental data. This study highlighted FDS's efficacy in modelling plume interactions and ambient conditions, providing valuable insights into wildfire dynamics. These validations underscore the robustness of FDS in modelling various wildfire scenarios, advancing its credibility as a tool for fire research. Gupta et al. [24] validated FDS 6.9.1 by comparing single pine tree simulation results with experimental HRR and MLR. Based on their study and the thermo-physical properties of the pine tree used, we adopted these properties for our pine forest simulations in the current study. A sensitivity analysis is carried out with another set of thermo-physical properties.

Despite the progress in understanding crown fire behaviour, there is a need for comprehensive field-scale simulations to better capture the impact of interactions between key factors such as CBH and wind speed. Previous studies have examined these variables independently or in small-scale simulations, but their combined effects on fire transition remain underexplored. This study aims to fill this gap by conducting field-scale, physics-based simulations using FDS to examine the threshold conditions for fire transition from surface to crown fire. We focus on two critical parameters—CBH and wind speed—and their interactions across different scenarios. The primary objectives of this study are to identify the threshold conditions for sustained and intermediate crowning, to investigate how crown base height and wind speed influence the likelihood of crown fire transition, and to compare the simulation results with existing models, such as those developed by Cruz et al. [20], to assess their predictive accuracy. In this study, crowning is defined as sustained flame propagation through the crown layer, indicated by both visual flame continuity and significant crown mass loss over a measurable duration.

2. Methodology

In our research, we will use FDS version 6.8 to conduct our simulations; the surface fuel will consist of pine needles, and the simulated forest ecosystem will be a pine forest. The forest is assumed to be rectangular with dimensions of 260 m long by 16 m wide, as presented in Fig. 1. The lateral boundaries were equipped with a mirror symmetry condition, where the spatial derivatives were set to zero, effectively mirroring the side boundaries to emulate an infinitely wide forest. While

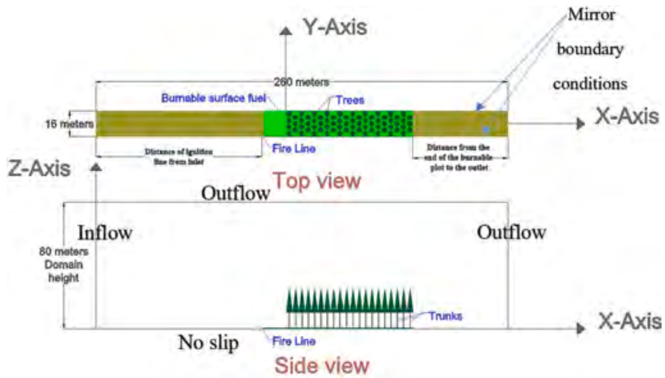

Fig. 1. Layout of the forest used in this study. The upper section illustrates the top view, while the lower section shows the side view.

this approach may suppress lateral wind variability and fire edge effects, it was selected to reduce computational cost and to maintain a focused analysis on the central fire behaviour. Given that the primary objective is to examine thresholds for crown fire transition under varying wind speeds and crown base heights, we expect that the influence of this assumption on the main conclusions is minimal. A numerical domain is considered, which extends from x = −120 m to x = 140 m in longitudinal direction, from y = −8 m to y = +8 m in spanwise direction, and from the ground (z = 0 m) to a height of 80 m. A fire line (red coloured) represents the line ignition source at x = −15 m, near the upwind edge of the fuel bed, to ensure consistent and repeatable fire initiation across all cases. The burnable surface fuel starts 105 m (i.e, from the fireline x = −15m) from the inlet to ensure well-developed turbulence (which is equivalent to more than 3x-7x tree heights considered in the present study). A 17-m distance was maintained between the ignition line and the centreline of the first row of trees. This spacing was determined through preliminary simulations and was found to be adequate for allowing the surface fire to reach a steady propagation rate before interacting with the crown fuel.

The dark green cones represent our forest trees (crown fuel), while the light green area represents the pine needles (burnable surface fuel). Fuel placement was based on a uniform distribution to isolate the effects of the studied parameters (e.g., CBH and wind speed) without introducing spatial variability. Pine trees are evergreen, coniferous, resinous trees and occasionally shrubs that typically reach heights of 3–80 m, depending on their age. In this study, we will simulate trees of two different age groups to examine how changes in crown base height (CBH) influence fire transition. Since CBH is related to the overall tree height, altering the CBH also affects the forest age.

We conducted simulations for forests with CBHs of 1 m, 5 m, and 10 m, corresponding to total tree heights of 12 m, 17 m, and 25 m, respectively. This data is obtained from Cruz's guide [28], which describes radiata pine plantations at various growth stages commonly found in south-eastern Australia, particularly in regions like Victoria and New South Wales. For an older forest with a CBH of 15 m and tree height of 30 m, initial simulations showed no transition from surface to crown fire, as the high CBH was a key factor preventing the transition. However, such transitions do occur in real-world scenarios. This discrepancy may be attributed to limitations in the simulation setup, including the absence of ladder fuels, insufficient representation of turbulence, challenges in fully idealizing real-world conditions, limitations in resolving fine-scale fuel elements, and inadequate representation of temporal and spatial variability, all of which are inherent constraints of the physical model used in the simulations. To explore this further, we adjusted the CBH of this forest to 10 m and the total tree height to 25 m. These adjustments helped us investigate the influence of CBH on fire transition, as discussed in the results section. The tallest forest in our simulations reaches 25 m, so we selected a domain height of 80 m, which is over three times the forest height, as recommended by Bou Zeid et al. [29]. The horizontal domain length should be at least four times the domain height to allow eddies to evolve before exiting the domain. In our simulations, we went slightly below this limit to ensure the fire develops naturally without being artificially confined, but still yield computationally tractable simulations.

In pine plantations, surface fuel loads from the literature typically range between 2 kg/m^2 [22] to 3.5 kg/m^2 [30], with some studies reporting values as high as 4.34 kg/m^2 [31]. Our surface fuel load is 5.4 kg/m^2, approximately 25 % greater than the highest values reported; however, we found this was necessary to achieve a simulated fire intensity sufficient to gain non-negligible crown mass loss in high CBH forests. The higher surface fuel load compensates for the lack of ladder fuels in the simulation. It also aims to represent a worst-case scenario for bushfires in such forests. A similar modelling approach that excluded ladder fuels was adopted by Moinuddin and Sutherland [26], where the focus was on isolating key drivers of crown fire behaviour under simplified fuel structures.

Wind speed is one of the key factors we aim to evaluate its impact on surface fire transition. We selected a wide range of open wind speeds measured at a 10 m height: 3 m/s, 6 m/s, 8 m/s, and 10 m/s, corresponding to 10.8 km/h, 21.6 km/h, 28.8 km/h, and 36 km/h, respectively. This range allows us to observe the effects of both low and high wind speeds on fire transition in forests with varying CBHs. In this paper, we will use a fixed moisture content of 5 % for all simulations, providing a controlled environment to understand the interested parameters better. Moisture content is influenced by relative humidity and ambient temperature. According to Cruz et al. [32], a moisture content of 5 % in pine forests corresponds to a relative humidity of 17 % and an ambient temperature of 37 °C. According to McArthur [33], with these humidity and temperature of air, the wind speeds correspond to Forest Fire Danger Index (FFDI) values of 70, 90, 110, and 130, respectively. While the Australian Fire Danger Rating System (AFDRS) has recently replaced the traditional McArthur-based FFDI for operational use, the FFDI remains widely used in research settings due to its transparency and reproducibility. The AFDRS employs a modular Fire Behaviour Index (FBI) that integrates advanced models, vegetation-specific fuel data, and high-resolution meteorological inputs. However, due to the complexity of the AFDRS framework and the limited public availability of its calculation tools, it was extremely difficult to directly compute FBI values for the current cases. As such, the McArthur-based FFDI was used as a reference to contextualize fire weather severity in a manner consistent with previous studies.

The trees are arranged in 20 lines, perpendicular to the x-direction, in an area of 80 m x 16 m in a staggered Fashion: the odd-numbered lines will have four trees, and the even-numbered lines will have three trees, as shown in Fig. 1. It can be reminded that due to setting the mirror symmetry condition on the lateral boundaries, the tree settings can be considered an infinitely wide forest. The tree centres and the spaces between lines maintain a 4-m distance, so the total number of trees is 70. The outflow and top boundaries were set as open to allow unobstructed movement of wind and combustion gases, including smoke, with a constant pressure specified at these boundaries. Side boundaries were set as mirror, as previously mentioned, while the bottom boundary was treated as solid ground with no-slip conditions. These boundary conditions were selected to ensure realistic airflow development, enable wind-driven fire to spread, and prevent artificial confinement of the fire plume. The inflow boundary was configured to provide a steady wind profile appropriate for each scenario.

We divided the domain into subdomains for parallel computing and adopted appropriate grid sizes in the near-field and far-field. FDS automatically calculates the time step size to ensure the Courant–Friedrichs–Lewy (CFL) number remains within the range of 0.8–1.0 [27]. Table 1 shows the thermo-physical properties used in our simulation for the surface fuel and the crown fuel.

We used the VLES sub-model in FDS for turbulence modelling [34].

Table 1
Thermo-physical, pyrolysis, and combustion parameters for the fuel.

Fuel type	Fuel Parameter		Values	Reference
Surface fuel (Pine needles)	Fuel load		5.4 kg/m^2	[31]+ 24 %
	Moisture content		5 %	Simulated condition
	Air temperature		37 °C	[32]
	Relative humidity		17 %	[32]
	Surface area to volume ratio		4661 m^{-1}	[22]
	Density		650 kg/m^3	
	Heat of Combustion		17700 kJ/kg	
	Thermal conductivity		100 W/m. K	
	Pre-exponential factor A (dry vegetation)		1.18E+03 s^{-1}	
	Activation Energy E (dry vegetation)		6.58E+04 J/mol	
	Pre-exponential factor *A* (moisture)		4.83E+03 s^{-1}	
	Activation Energy *E* (moisture)		3.91E+04 J/mol	
Crown fuel (pine trees)	Moisture content		5 %	Simulated condition
	Crown fuel load		1 kg/m^2	[28]
	Heat of Combustion		36712 kJ/kg	[24]
	needles	Mass fraction	15.04 %	
		Surface area to volume ratio	2040 m^{-1}	
		Activation Energy (E)	326 E3 J/mol	
		Pre-exponential factor (A)	3.163E24 m/s	
		Density	390 kg/m^3	
		Thermal conductivity	0.15 W/m. K	
	needles thin	Mass fraction	45.16 %	
		Surface area to volume ratio	4040 m^{-1}	
		Activation Energy (E)	326 E3 J/mol	
		Pre-exponential factor (A)	3.163E24 m/s	
		Density	390 kg/m^3	
		Thermal conductivity	0.15 W/m. K	
	less-than-3mm	Mass fraction	6 %	
		Surface area to volume ratio	1640 m^{-1}	
		Activation Energy (E)	326 E3 J/mol	
		Pre-exponential factor (A)	3.163E24 m/s	
		Density	390 kg/m^3	
		Thermal conductivity	0.15 W/m. K	
	3 mm–6mm	Mass fraction	10.7 %	
		Surface area to volume ratio	1000 m^{-1}	
		Activation Energy (E)	254E3 J/mol	
		Pre-exponential factor (A)	5.01E18 m/s	
		Density	440 kg/m^3	
		Thermal conductivity	0.26 W/m. K	
	6 mm–10mm	Mass fraction	17.6 %	
		Surface area to volume ratio	500 m^{-1}	
		Activation Energy (E)	254E3 J/mol	
		Pre-exponential factor (A)	5.01E18 m/s	
		Density	440 kg/m^3	
		Thermal conductivity	0.26 W/m. K	
	10 mm–15mm	Mass fraction	5.5 %	
		Surface area to volume ratio	333 m^{-1}	

Table 1 (*continued*)

Fuel type	Fuel Parameter		Values	Reference
		Activation Energy (E)	270E3 J/mol	
		Pre-exponential factor (A)	1.99E19 m/s	
		Density	590 kg/m^3	
		Thermal conductivity	0.18 W/m. K	
	Fuel Geometry		cone	[26]
	Cone height		Changed according to simulated age	
	Cone radius		2 m	Simulated condition
Char	Pre-exponential factor A_{char} (Char oxidation)		465 m/s	[35]
	Activation Energy E_{char} (Char oxidation)		68000 J/mol	
	Density		300 kg/m^3	
	Thermal conductivity		0.05 W/m. K	

The VLES model (the default in FDS 6.8.0) provides a compromise between the physical faithfulness of LES and computational feasibility; the fine grid required by LES with other subgrid-scale turbulence models is not feasible. However, VLES has limitations in capturing fine-scale turbulence, particularly in regions of strong shear and entrainment, such as near the crown base. This may lead to underpredicted localized mixing and entrainment rates, potentially affecting flame attachment and vertical fire propagation. Despite these limitations, VLES remains a suitable choice given the large domain and the need to simulate multiple scenarios [27]. We conducted a comparison of two different turbulence models—LES and VLES—for two representative cases: CBH10W8 and CBH10W10 using the same grid resolution of 0.25 m and observed minor differences in the peak values s for both the heat release rate per unit area and the mass loss rate. However, the overall trend and fire behaviour remained consistent throughout the entire simulation for both models.

We used the FDS' Fuel Element (FE) sub-model, which is suitable for representing vegetation occupying specific volumes, such as trees. This model necessitates a gas phase grid with adequate resolution to accurately depict temperature gradients and heat exchange between the gas and solid phases, as outlined in the FDS technical guide [34]. In our simulation, the FE sub-model is used for both the surface and crown fuels (trees).

Before conducting the parametric simulations, we performed a sensitivity analysis to determine appropriate values for key parameters, including gas-phase grid resolution, domain height, the distance between the ignition line and the inlet, the distance from the end of the burnable plot to the outlet, and the intensity of the ignition line. We selected a case with a CBH of 10 m and a wind speed of 8 m/s to conduct this analysis for each parameter. We will present the sensitivity analysis for the grid size, while the analyses for the other parameters will be included in Appendix A.

In our sensitivity analysis of the grid size, we simulated three cases with different grid sizes—0.25 m, 0.33 m, and 0.5 m—for the sensitive area of the domain (x = −20 m to x = 100 m), which contains the vegetation. For the less sensitive areas, we used a grid size twice that of the sensitive region. By comparing the heat release rate (HRR) and mass loss rate (MLR) across the three cases, we found no significant difference in HRR between the 0.25 m and 0.33 m grid resolutions. However, the simulation with a 0.5 m grid size showed markedly different behaviour, as illustrated in Fig. 2(a). For the MLR, there were slight differences in peak values across all three cases. Notably, between 230 and 320 s, the 0.5 m grid case diverged significantly from the other two, as shown in Fig. 2(b).

Based on the observed comparison and the similarity in results between the 0.25 m and 0.33 m grid cases, there is no need to perform

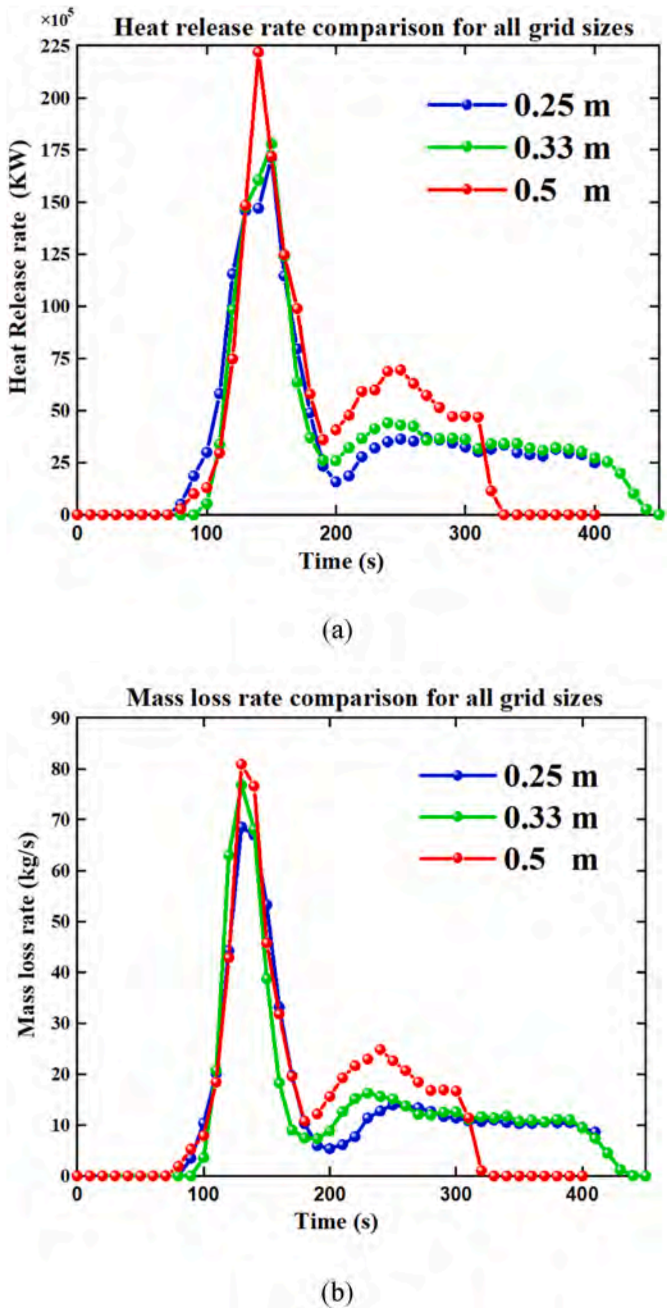

Fig. 2. (a) Comparison of HRR and (b) MLR for three cases with different grid sizes.

simulations with a grid resolution finer than 0.25 m. In choosing between the 0.25 m and 0.33 m grid sizes, we selected 0.25 m to align with Morvan's study [36], which recommends 0.25 m as the appropriate extinction length scale for pine forests; he also stated that the grid size for Particle Model simulations should be equal to or smaller than the extinction length. Moinuddin and Sutherland [26] also used 0.25 m after a grid sensitivity study. Furthermore, using the 0.25 m grid instead of 0.33 m enhances the ability to capture complex physics more realistically and resolves turbulent structures and smaller eddies with greater accuracy. Therefore, we will use a 0.25 m grid for the vegetated areas and a 0.5 m grid for the non-vegetated areas in our simulations.

The sensitivity analysis for the remaining parameters indicated that the optimal values for domain height, the distance between the ignition line and the inlet, the distance from the end of the burnable plot to the outlet, and the initiating ignition line intensity are 80 m, 105 m, 60 m, and 2000 kW/m^2, respectively. For detailed results and the methodology of the sensitivity analysis, please refer to Appendix A. It is to be noted that the initiating ignition line intensity of 2000 kW/m^2 resulted in the surface fire intensity of approximately 5158.7 kW/m when it approaches the edge of the forest. This value is influenced by the characteristics of the fuel bed. In our study, each case is labelled as CBH (Crown Base Height) W (Wind Speed), where, for example, CBH5W6 denotes a case with a crown base height of 5 m and an open 10-m height wind speed of 6 m/s. The simulation scripts are almost identical for all cases, with the only variations being to the CBH and wind speed.

3. Results and discussion

3.1. Visual observation

The results of the simulations are visually summarised in Fig. 3 using FDS' companion visualization software Smokeview, which provides two key renderings for each case. The left screenshot captures the moment when the surface fire begins to interact with the crown vegetation, while the right one illustrates the state near the end of the simulation.

In the case of CBH10W3, with the lowest wind speed of 3 m/s (Fig. 3(a)), we visually observe no sustained crowning. The images show that the fire reaches within the crowns but with minimal crown particle removal (burn-away) by the end of the simulation. When the wind speed increased to 6 m/s in case CBH10W6 (Fig. 3(b)), we initially observed a forward inclination of the flame and higher penetration of the flame within compared to CBH10W3. However, by the time the flame reaches the forest end, it is barely touching the crown particles. We can observe a noticeably greater number of crown particle burn-away compared to the case with a wind speed of 3 m/s; however, these are limited to 2–3 rows of pine trees.

In case CBH10W8, with a wind speed of 8 m/s, we observe in Fig. 3(c) an elongated surface fire at the beginning. At a later stage, only the tip of the flame is observed to touch the bottom of the crown particles. A larger number of particles burn away is compared with the cases with 3 m/s and 6 m/s wind speeds (but limited to 3–4 rows of pine trees). Please also note the colour change of particles into maroon and yellow, which also reflects particle mass loss, though not full burn away. At 10 m/s wind speed case CBH10W10 (Fig. 3(d)), further elongated surface fire is observed. More particles burn away are observed compared to the 8 m/s case in the forest's middle, but quickly move past without further crown particle burning with reduced flame height. Overall, these cases demonstrate that crown particle burn-away is insignificant for CBH 10 m, particularly at very low (3 m/s or lower). The observations indicate that a CBH of 10 m significantly limits the likelihood of crowning under various wind conditions.

By moving to another series of simulations with CBH of 5 m, we observe that at the impact region, flames rise above the forest crown in case CBH5W3, with lower wind speeds of 3 m/s (Fig. 3(e)). Flame heights are observed to significantly diminish when the flame reaches the forest end edge. While particle burnway is observed at the impact region in Fig. 3(e)–ie, CBH5W3 case, in CBH5W6 case (Fig. 3(f)), more particle burnway is observed a little downstream of the impact region, indicating a heightened probability of crowning. In CBH5W3, we can observe particles turning yellow at the bottom part of the forest crown. Increasing wind speed from 3 m/s to 6 m/s shows more particles turning yellow in the upper part of the crown.

However, with further increases in wind speed to 8 m/s (CBH5W8) and 10 m/s (CBH5W10), we observe a deep inclined flame within the forest crown at the impact region (also in the CBH5W6 case). As the flame travels downstream, a second significant flame rise within the forest crown occurs (see colour change of particles into maroon), and when the flame reaches the forest end, the flame tip is in the middle of the forest crown. Particle burning becomes nearly consistent across these higher wind speeds. Overall, for a CBH of 5 m, the particle burning appears to be substantial.

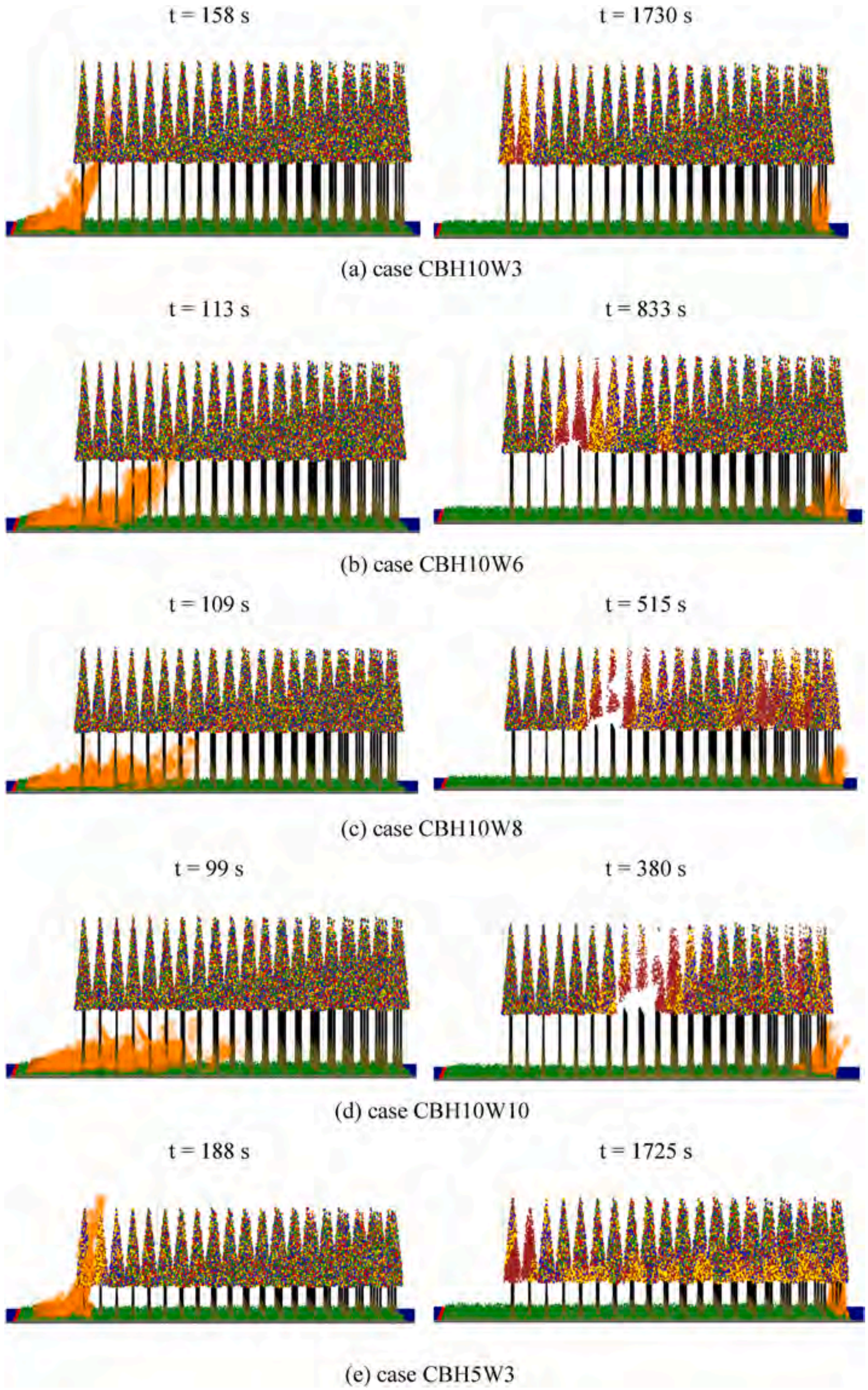

Fig. 3. Some Smokeview screenshots for the simulated cases. The left side of each image shows the moment when the surface fire begins interacting with the crown vegetation, while the right side depicts the state near the end of the simulation. The time at which each screenshot was taken is indicated above the corresponding image.

The next series of simulations with a CBH of 1 m reveals a dramatic increase in crown particle burning, depicting clear cases of crowning at this low CBH. Fig. 3(i) related to case CBH1W3, with a wind speed of 3 m/s, shows that most crown particles along the bottom part of the forest crown turned into maroon and yellow. Increasing the wind speed to 6–10 m/s, we observe a massive loss of crown particles across the forest region (complete burn-away and turning into mostly maroon colour).

3.2. *Mass loss of forest crown during fires*

Fig. 4 illustrates the crown mass loss across all simulated cases. In this study, *crown mass loss* refers to the percentage reduction in crown fuel mass over time due to burning, as tracked using the PARTICLE output. The case with the lowest wind speed and highest CBH does not exhibit crown fire, resulting in minimal crown mass loss (CBH10W3). In

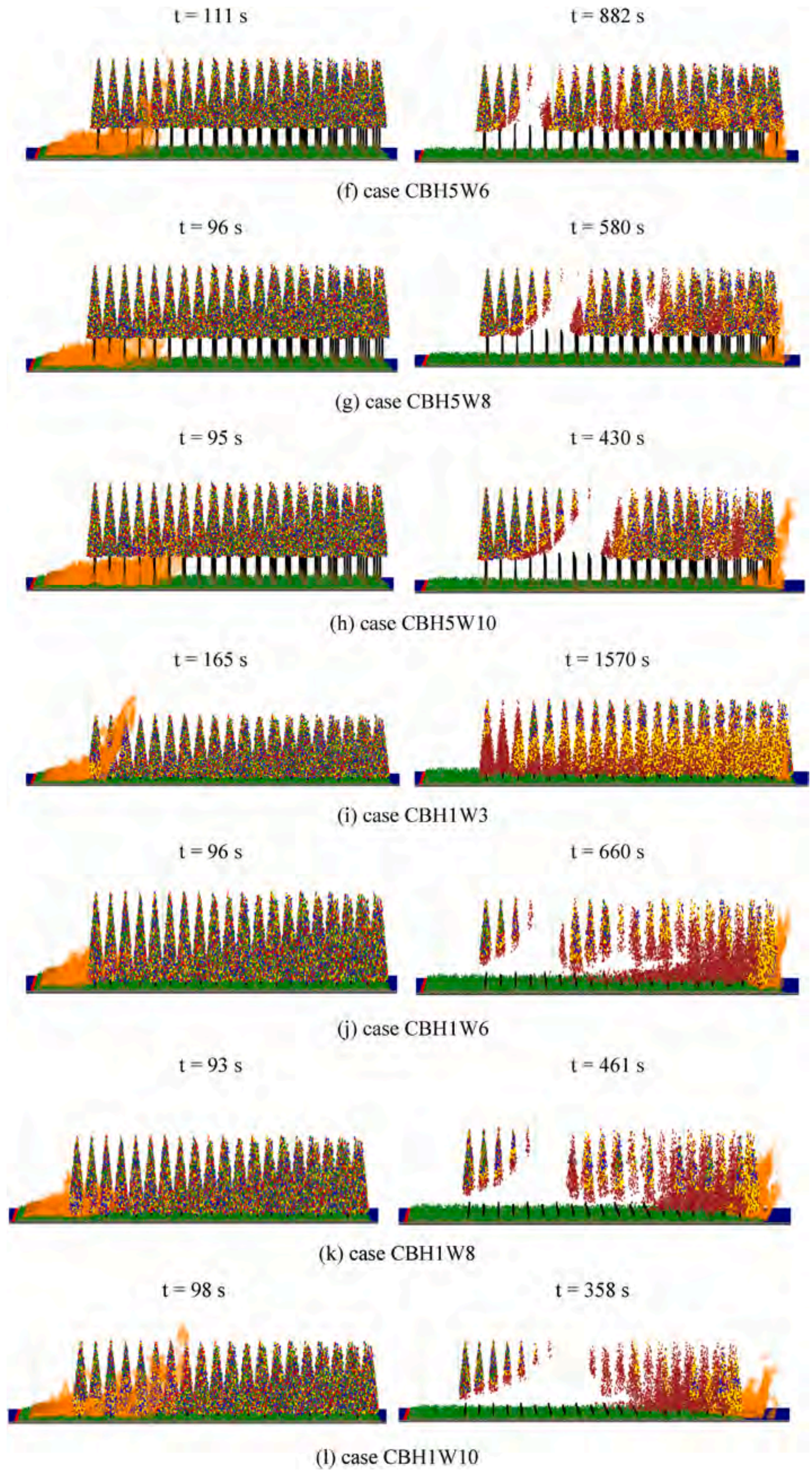

Fig. 3. (*continued*).

contrast, the cases with the lowest CBH with all wind speeds show nearly complete crown mass loss, indicating crown fire.

It is also evident that, with CBH = 10 m, increasing the wind speed leads to a corresponding increase in the mass loss. The increased mass loss rate is likely due to the increased convective heat transfer and flame penetration into the crown layer under higher wind conditions,

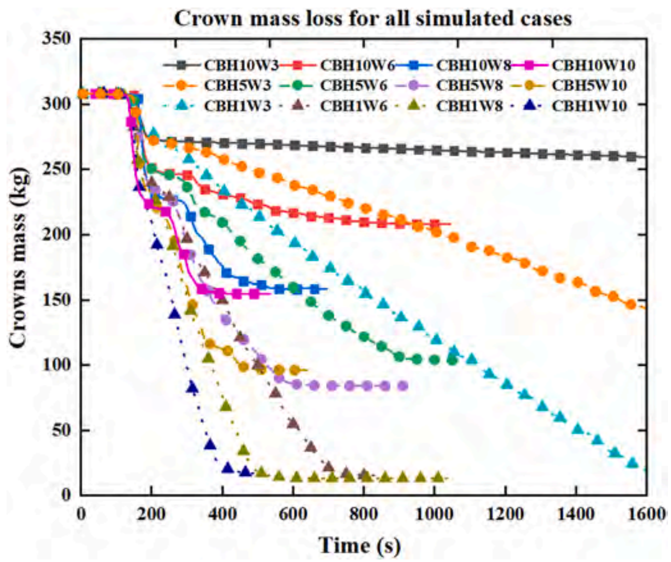

Fig. 4. The crown mass loss for all simulated cases. The curves with rectangular symbols and solid lines represent cases with a CBH of 10 m, while those with circular symbols and dash lines correspond to a CBH of 5 m. Similarly, the curves with triangular symbols and dot lines denote cases with a CBH of 1 m.

accelerating the combustion of crown fuels. It is to be noted that as higher wind speeds accelerate fire spread, reducing the residence time. However, convective heat transfer and flame penetration overcome the effect of the lower residence time. It can also be observed that, as wind speed increases, the crown mass loss rate also increases (for all CBHs). However, for other simulation series with CBH 5 m and 1m, total mass loss does not vary much.

Fig. 5(a) depicts the crown mass loss % for each simulated case, while Fig. 5(b) shows the corresponding time required for this mass loss. Within each simulation series with a fixed CBH, increasing the wind speed leads to a reduction in the time required for crown mass loss. Furthermore, lower CBHs consume less time than higher CBH cases at the same wind speed. This is because the crown is closer to the surface fire, allowing the flames to reach the crown more easily and quickly, reducing the time required for the fire to transition from surface to crown.

We can correlate crown mass loss % data with the visual representations of Fig. 3. With CBH = 10 m, the mass losses were 16.2 %, 32.5 %, 48.6 %, and 49.8 % for 3, 6, 8, and 10 m/s wind, respectively. This is reflected in Fig. 3(a–d), which depicts considerable particle burn-away for 6–10 m/s cases compared to the CBH10W3 case. Despite above 45 % mass loss, we observe that it is insufficient to sustain crowning.

In the next series of simulations with CBH of 5 m, in case CBH5W3, with a low wind speed of 3 m/s, crown mass loss reached 58.9 %, significantly higher than the 16.2 % observed in CBH10W3. This highlights the role of reduced CBH in enhancing mass loss and increasing the likelihood of crowning. However, particle presentation snapshots in Fig. 3(e) do not display significant particle drops as seen in cases with CBH 10 m, but this is due to our Smokeview visualization technique. The representation uses six colours to depict crown vegetation, and vegetation loss is inferred not only from the appearance of white regions but also from the reduction in coloured points or a colour change to maroon and yellow, especially in the case of CBH5W3. In this case, while no white areas are visible, a substantial reduction in coloured points or a colour change reflects significant vegetation loss, particularly from the lower half of the crown, where loss is expected to be greater than from the upper half. As wind speed increased to 6 m/s in case CBH5W6, mass loss rose further to 66.3 %, indicating a heightened probability of crowning. Further increases in wind speed to 8 m/s (CBH5W8) and 10 m/s (CBH5W10) led to slight increases in crown mass loss, at 72.7 % and 68.7 %, respectively. The crown mass loss at 10 m/s was lower than at 8 m/s. This may be attributed to the effect of very high wind speeds pushing the surface fire closer to the ground, thereby reducing its interaction with the crown vegetation. These findings are consistent with the observations reported by Scott [8]. In the series of simulations with a CBH of 1 m, a drastic increase in crown mass loss is observed. In all cases, crown mass loss reached ~95 %

For different tree species, sustained crowing may occur at different CBH and wind speeds. For fire behaviour, a tree species is predominantly defined by its thermo-physical properties. Therefore, we repeated the above simulations for species with different thermo-physical properties. In the modified thermo-physical properties, we used five crown fuel particles instead of six and adjusted the fuel heat of combustion and char properties. Modifications were made, and their impact on fire behaviour was analysed. Table 2 compares the physical properties used in the modified series with those from the main series.

In the modified series, the crown mass loss increased across all cases compared to the main series. For cases with a CBH of 1 m, the crown vegetation is located very close to the surface fire, resulting in a higher percentage of mass loss; however, the overall mass loss pattern remained largely unchanged. In cases with CBH of 10 m, the general pattern also remained unchanged. This is likely due to the higher distance between the surface fire and crown vegetation, which limited particle removal from the canopy and reduced the overall crown mass loss. In contrast, cases with CBH = 5 m exhibited a notable difference in both the amount and pattern of crown mass loss. Therefore, only the results for CBH = 5 m are presented in the main text, while results for CBH = 1 m and 10 m are provided in Appendix B.

In Fig. 6, we observe that at the impact region, flames rise above the forest crown in cases CBH5W3 and CBH5W6, corresponding to lower wind speeds of 3 and 6 m/s (Fig. 6a and b). Flame heights significantly diminish as the flames reach the forest edge. While particle burn-away is observed at the impact region in Fig. 6(a) (CBH5W3), in Fig. 6(b) (CBH5W6), more particles burn-away occurs downstream of the impact region, indicating a heightened probability of crowning. However, with further increases in wind speed to 8 m/s (CBH5W8) and 10 m/s (CBH5W10), we observe deeper flame penetration within the forest crown at the impact region. As the flames travel downstream, a second significant flame rise occurs within the forest crown. By the time the flames reach the forest's edge, the flame tip is positioned in the middle of the forest crown. Particle burn-away becomes nearly consistent across these higher wind speeds. Overall, for a CBH of 5 m, particle burn-away appears to be substantial. Increasing wind speed from 3 m/s to 6 m/s enhances flame penetration and burning rates, facilitating the transition from surface to crown fire and increasing the probability of crowning.

Fig. 7 (a) presents the crown mass loss for cases with a CBH of 5 m from both the main and modified series, while Fig. 7 (b) shows the corresponding percentage of crown mass loss. It is evident from Fig. 7 (a) that the rate of mass loss in the modified series is higher than that in the main series. As shown in Fig. 7 (b), the crown mass loss percentages in the modified series were 78.06 %, 84.29 %, 83.67 %, and 82.59 % for wind speeds of 3 m/s, 6 m/s, 8 m/s, and 10 m/s, respectively. The corresponding durations required to reach these losses were 1170 s, 745 s, 505 s, and 385 s. All these percentages exceed those observed in the main series. The crown mass loss slightly decreased as wind speed increased from 6 m/s to 10 m/s. This reduction may be attributed to the same effect discussed in Fig. 5(a), where higher wind speeds may push the surface fire closer to the ground, thereby reducing its interaction with the crown vegetation.

Based on these results and the particle presentation in Figs. 3 and 6, we can infer that a sustained transition from surface to crown fire occurs in cases where crown mass loss reaches 80 % or higher. Cases with crown mass loss between 65 % and 80 % can be classified as intermediate crowning, while those below this threshold exhibit an incomplete transition. According to this classification, in the modified series, CBH5W3 falls under intermediate crowning, while CBH5W6, CBH5W8,

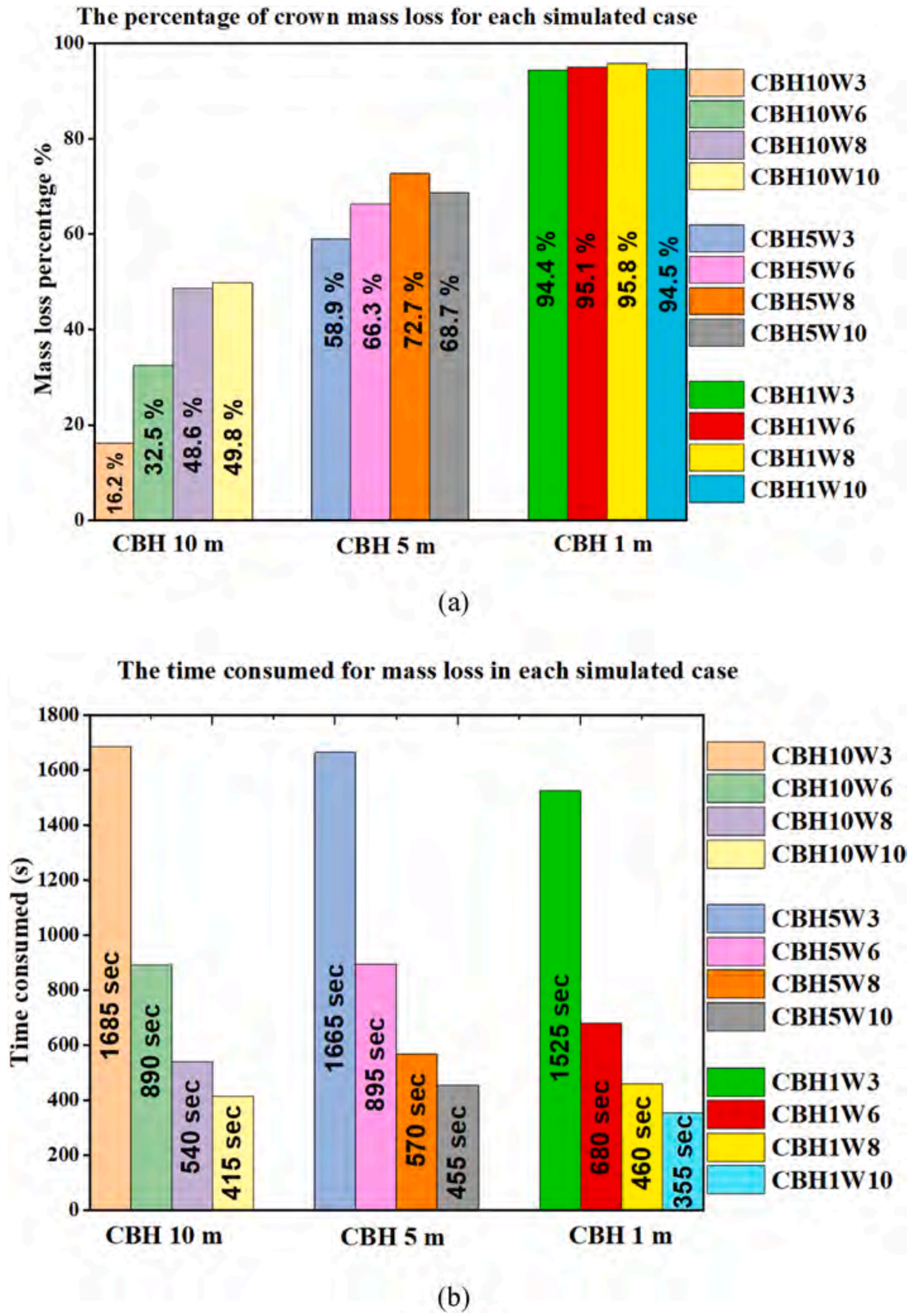

Fig. 5. (a) Percentage of crown mass loss for each simulated case. Cases with lower CBH exhibit nearly complete mass loss, indicating crown fire, while cases with intermediate CBH show similar effects but with a lower percentage of mass loss. The case with the highest CBH exhibits the lowest mass loss, suggesting a very low probability of crown fire. (b) Crown mass loss duration for each case. As wind speed increases, the duration of crown mass loss decreases.

and CBH5W10 exhibit sustained crowning. In contrast, in the main series, CBH5W3 corresponds to an incomplete transition, while the other cases are classified as intermediate transition.

3.3. Streamline analysis of simulated cases

Visualising the flame contours, temperature contours, and wind velocity vectors along the centreline of the forest plot at various time instances is particularly useful for understanding flame behaviour. The wind velocity vectors are utilized to visualize the flow patterns and capture the dynamic behaviour as the fire progresses. This dynamic behaviour arises from pressure differentials between the zones upstream and downstream of the flame, as reported by Refs. [37,38]. The vectors provide an instantaneous depiction of flow direction, offering insight into turbulence at specific moments in time. To thoroughly understand entrainment trends, an ensemble average of the wind field as the fire evolves would need to be generated. However, such analysis is beyond the scope of this study. Eftekharian et al. [38] observed in their simulation that the strongest fire-induced pressure gradient occurs in the low-density region immediately downstream of the fire source, leading to maximum wind enhancement. This enhancement gradually diminishes along the plume line as it extends further downstream from the fire, a pattern also observed in our results. Each simulation generates a unique stream plot at every time step. For practicality, we present two key stream plots for each case: one at the time of maximum heat release rate (HRR) and another shortly before the end of the simulation. Due to

Table 2
Differences in thermo-physical properties between the modified and main series.

Fuel		Modified Series	Main Series
Crown needlesthin	Mass fraction	No Crown needlesthin used in this series	45.16 %
	Surface area to volume ratio		4040 m^{-1}
Crown needles	Mass fraction	60.2	15.04 %
	Surface area to volume ratio	2040 m^{-1}	2040 m^{-1}
Surface Heat of Combustion		18000 kJ/kg	17700 kJ/kg
Crown Heat of Combustion		18000 kJ/kg	36712 kJ/kg
Char	Pre-exponential factor A_{char} (Char oxidation)	430 m/s	465 m/s
	Activation Energy E_{char} (Char oxidation)	74800 J/mol	68000 J/mol
	Density	300 kg/m^3	300 kg/m^3
	Thermal conductivity	0.052 W/m.K	0.05 W/m.K

reduced turbulence near the end of the simulation, we focus on the downstream section of the forest, from x = 60 m to x = 100 m, covering only the end portion of the vegetation.

In contrast, the stream plot at the peak HRR moment displays the entire vegetation area, from x = −20 m to x = 100 m. This approach highlights both the peak flow behaviour and the final flow conditions. Fig. 8 displays these streamline plots on the XZ plane.

The plots show flame contours (red) with a temperature colour map shaded in the background, wind vectors (white arrows), and white lines indicating areas with zero U velocity. On the left and above the white lines, we observe forward flow driven by convection (may include some entrainment), and on the right and below, reverse flow represents entrainment. Additionally, the vertical white lines near the ground represent tree trunks, where no more flow occurs around them. Examining the areas enclosed by the red lines in each streamline plot presented in Fig. 8, which represent the flames, reveals that as wind speed increases, the longitudinal diameter of these areas also increases. This trend indicates that higher wind speeds expand the area of crown vegetation impacted by flames originating from the surface fire, thus increasing the likelihood of more crown vegetation igniting. This is also observed in Figs. 3 and 6.

3.4. Flame height assessment

Flame height is a key factor in describing the transition from surface fire to crown fire in each case. It is well-established that when the flame height is sufficient to penetrate the crown, the transition to crown fire is more likely to occur due to heating the lower parts of the crown. Additionally, if the flame remains in the crown for an extended period (longer residence time), the transition becomes more sustained, resulting in a higher crown mass loss. The flame height, flame length, and flame angle are figured out by examining the HRR data from the slice file along the centreline at each moment (y = 0). This centreline was selected as a representative vertical plane, as only minor lateral flame fluctuations were observed across the domain, suggesting that the centreline provides a reliable approximation of overall flame behaviour. At every time step, we analyse the HRR data and use the highest observed HRR value as a threshold value to create a black-and-white image. In this image, areas inside the threshold value boundary are marked as one, and those outside are marked as zero. Following the approach of Cobian-Iñiguez et al. [39], we use MATLAB to fit an ellipse to this binary image at each time step. This ellipse is fitted using the moments of the nonzero

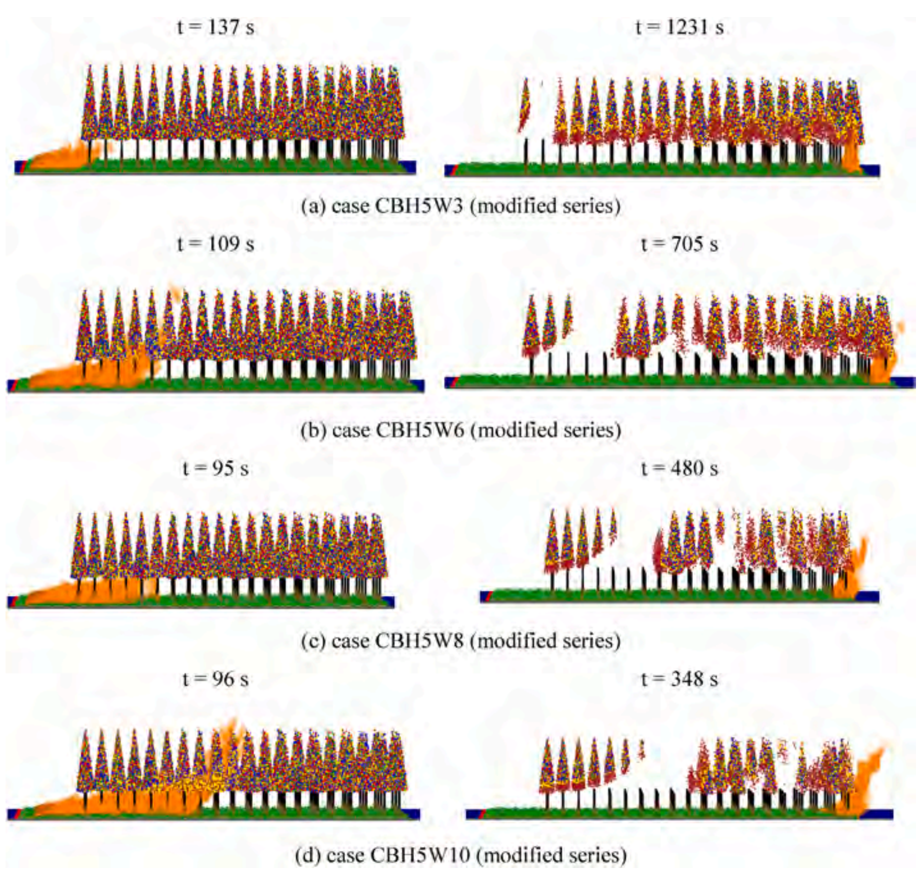

Fig. 6. Some Smokeview screenshots for the simulated cases with modified properties and CBH = 5m.

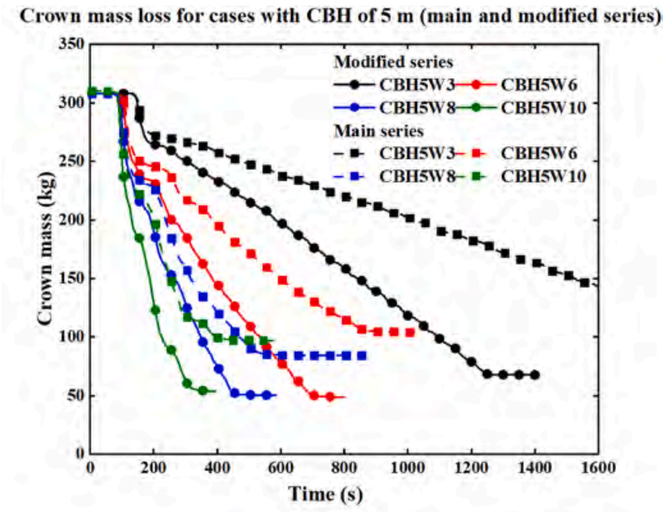

(a)

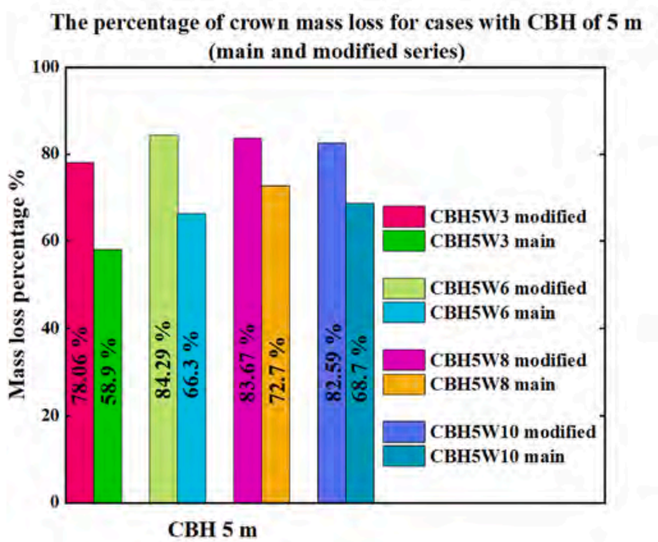

(b)

Fig. 7. (a) Comparison of crown mass loss for cases with a CBH of 5 m between the main and modified series. The curves with rectangular symbols and dash lines represent the main series, while those with circular symbols and solid lines correspond to the modified series. **(b) Comparison of the percentage of crown mass loss for the same cases.**

region in the image, ensuring its shape reflects the spread of the region. The flame length is then calculated based on the major axis of this fitted ellipse, representing the distance from the centre of the flame base to the tip of the flame. By calculating the minor axis, we can also determine the flame height and the flame angle.

Flame can help validate the threshold conditions of 80 % crown mass loss for sustained crowning and 65 % for intermediate crowning. Therefore, this section will focus on the analysis of flame heights across all simulated cases. Plotting the flame heights for all cases in a single graph would be too complex due to the intersection of curves, so they were separated into four plots in Fig. 9, corresponding to cases with the same CBH. In each plot, two horizontal lines represent the top of the crown and the bottom edge for that specific CBH, allowing the flame height curves between these lines to indicate the flame height inside the crown vegetation. The flame reaches the crown vegetation for a longer duration in cases with CBH = 5 m and CBH = 1 m, compared to CBH = 10 m. Additionally, in cases with CBH = 1 m and some cases with CBH = 5 m, the flame height reaches above the crown, increasing the likelihood of transitioning to crown fire. However, in CBH = 10 m, the flame height above the crown vegetation is minimal, indicating a lower chance of fire transition due to the limited flame penetration inside or above the crown in these cases.

By comparing Fig. 9(b) and (c) for the same CBH with different thermo-physical properties, we observe that cases with modified thermo-physical properties exhibit a higher flame height. In modified series, the flame remains in the crown vegetation for a longer duration, which is the primary reason for the increased crown mass loss.

The type of crown fire can be distinguished by considering flame residence time. In Table 3, each case is represented by three values: the lower value indicates the percentage of time the flame height is below the crown vegetation, the middle value shows the percentage of time the flame height is within the crown vegetation, and the upper value represents the percentage of time the flame height is above the crown vegetation.

Table 3 shows that cases with a CBH of 1 m or 5 m (main or modified property) exhibit a large percentage of time with flame heights within or above the vegetation. For a CBH of 1 m, there are no observed flame heights below the crown vegetation, indicating that the lowest flame height is above 1 m. Thus, low CBH (1 m) and intermediate CBH (5 m with main or modified series) facilitate significant crown fire transitions across all wind speeds, with most of the flame duration spent either within or above the crown vegetation. The percentage of time that flames remain beneath the vegetation for cases with CBH = 5 m (main series) is 28.28 % and 21.52 % for CBH5W6 and CBH5W10, respectively, both of which are classified as intermediate crowning. In the case of CBH5W8, this percentage is 39.3 %, also classified as intermediate crowning; however, in this instance, the flame residence time above and within the crown was sufficient to induce significant mass loss. Conversely, for CBH5W3, the percentage of time flames remained below the vegetation is approximately 38 %, corresponding to the lowest percentage of flame height above the crown and a crown mass loss of less than 65 %. Consequently, this case is classified as exhibiting unsustained crowning, as discussed in the previous section.

For cases with a CBH of 5 m in the modified series, we observe that the percentage of time flames remain beneath the vegetation is around 25 % or less, except for Case CBH5W3. This case also has the lowest percentage of flame height above the crown and a mass loss of less than 80 %, leading to its classification as exhibiting intermediate crowning, consistent with the previous findings.

Cases with a CBH of 10 m exhibit a lower percentage of flame duration within or above the crown vegetation compared with the other cases at lower CBH and the same wind speed, consistent with the observations from Fig. 9. Additionally, the percentage of time with flame heights above the crown vegetation is 0.29 % at a wind speed of 3 m/s and does not exceed 4 % at 10 m/s, indicating that a full crown fire transition has not occurred. This also suggests that, at lower wind speeds for this CBH, flames remain at lower levels beneath the crown vegetation for most of the simulation time, as these wind speeds are insufficient to achieve the high flame heights necessary to penetrate the crown layer.

The most important factor in Table 3 is the middle value, which represents the percentage of flame duration within the crown vegetation. Given the significance of this value, we have divided it into two separate values in Table 4. In Table 4, each case displays two values: the upper value indicates the percentage of flame time in the upper half of the crown vegetation. In contrast, the lower value represents the percentage of flame time in the lower half. The sum of these two values for each case is equal to the middle value presented in Table 3.

For cases with a CBH of 10 m, most of the flame height duration is observed in the lower half of the crown vegetation compared to the upper half. This indicates that flame heights in these cases exceed 17.5 m for only brief periods. In the modified series, for cases with CBH = 5 m, we observed that increasing wind speed reduces the ratio of flame

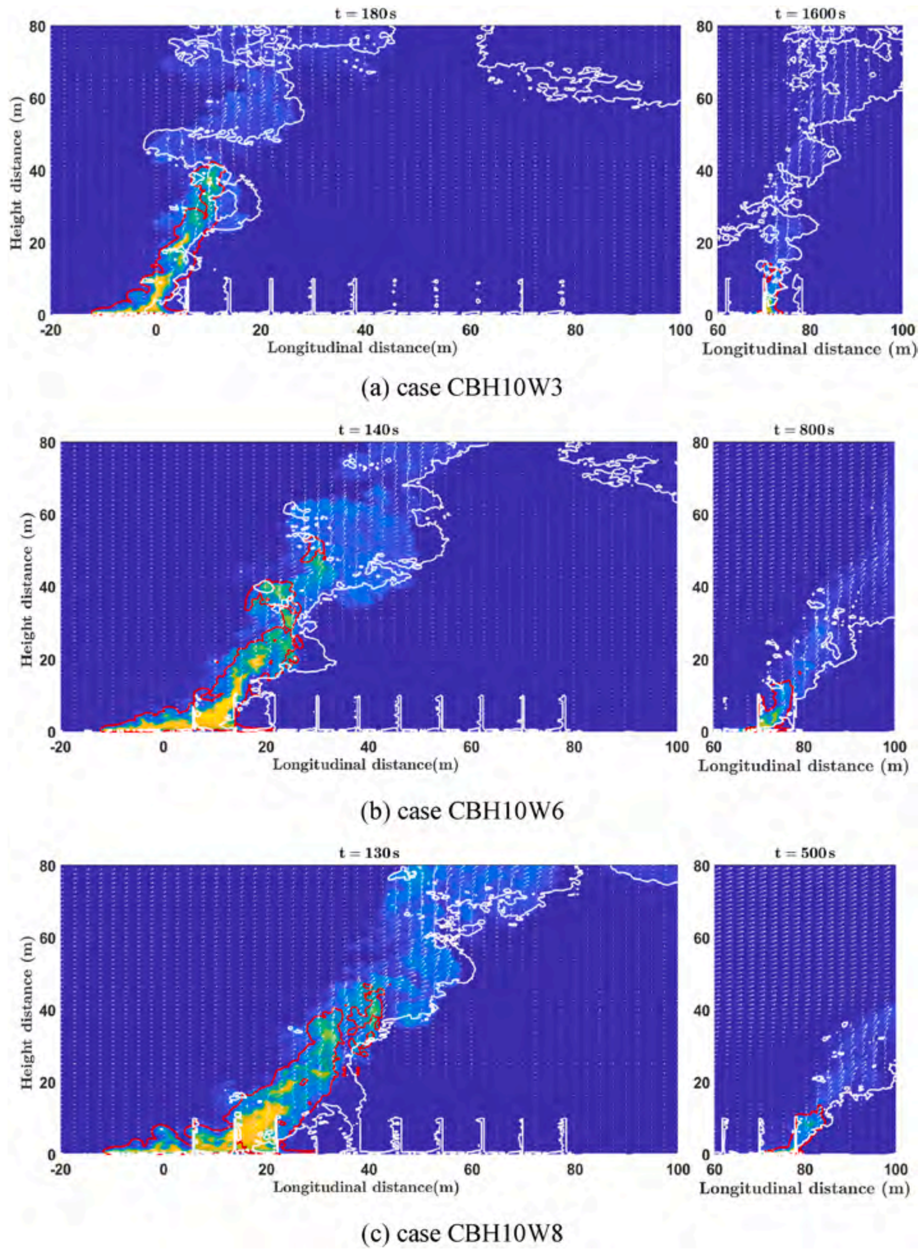

Fig. 8. Streamline plots for the XZ plane across simulated cases, showing red flame contours over a temperature colour map. White arrows indicate wind vectors, and white lines mark zero U velocity areas. The left side of each image captures the peak impact moment of the simulation, while the right side shows the conditions shortly before the simulation concludes. (For interpretation of the references to colour in this figure legend, the reader is referred to the Web version of this article.)

residence time between the lower and upper halves of the crown vegetation. Specifically, at a wind speed of 3 m/s, the ratio is 14, decreasing to 1 at 10 m/s. This suggests that at lower wind speeds, flames tend to persist longer in the lower part of the crown, while at higher wind speeds, flame residence time becomes more evenly distributed between the two halves. For comparison, in the main series, a similar trend is observed, but the ratio values differ. In Case CBH5W3 (main series), the flame height remains within the lower part of the crown vegetation for a duration nearly 41 times longer than in the upper part, indicating that at this lower wind speed, the flame height exceeds 11 m only briefly. As wind speed increases, this ratio decreases, reaching 1.14 at 10 m/s. In another case, CBH5W6 (main series), the flame remained within the crown vegetation for 70.88 % of the total duration (Table 3). Most of this time was concentrated in the lower portion (Table 4), with 66.24 % in the lower half and only 4.64 % in the upper half. This shows that the flame height was largely confined to the lower crown and did not fully penetrate the crown layer, which explains the relatively low crown mass loss observed in this case.

For cases with a CBH of 1 m, the ratio of flame time in the upper half of the crown vegetation to the lower half is 0.82 in one case and greater than 1 in two cases, with a slightly lower ratio of 0.4 in case CBH1W3. This indicates that flame heights at this CBH are sufficient to reach and remain above the crown vegetation for extended periods, primarily due to the lower forest height in these cases, which is the key factor contributing to sustained crowning at this CBH.

3.5. *Threshold model for crowning at 5 % moisture content*

In this section, we will present the critical values for the parameters that influence the transition from surface fire to crown fire in our

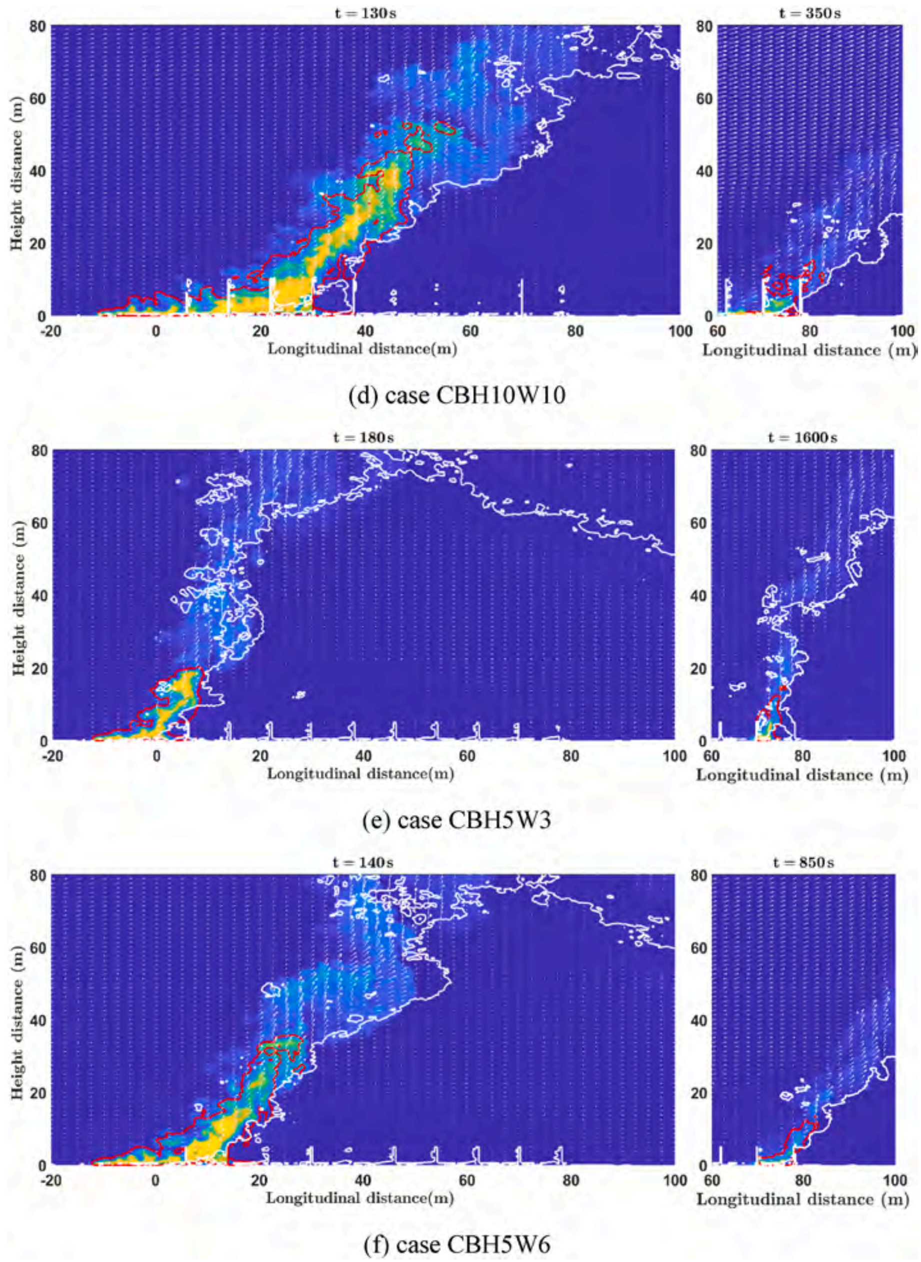

Fig. 8. (*continued*).

simulations. From the simulations conducted, it appears that if the crown mass loss is >80 %, it represents a sustained crowning, while values between 65 % and 80 % correspond to intermediate crowning. Flame contour and flame height analyses support this.

Regarding CBH, from our simulations, we can say the transition from the surface to the crown is highly dependent on the CBH. For CBH values of 10 m or more, no sustained crowning was observed over a wide range of wind speeds for the forest configuration and its thermo-physical properties, as seen in cases CBH10W3 through CBH10W10. However, for lower CBH values, such as in cases CBH5W6 through CBH1W10, we observed sustained or intermediate transitions from surface fire to crown fire.

The effect of wind speed on the fire transition appears to be CBH-dependent. For low CBH (e.g., 1 m), wind speed or thermo-physical properties do not significantly influence crowning behaviour, and this matches the observation from Grinshin and Perminov [10]. For CBH = 5 m (main series), we observed a crown mass loss exceeding 65 % in cases CBH5W6 through CBH5W10, while case CBH5W3, which featured the lowest wind speed, exhibited a reduced mass loss. Thus, lower wind speeds at CBH = 5 m appear to decrease the probability of sustained crowning, which matches the observation from Linn and Cunningham [7].

For CBH = 5 m in the modified series, we observed the same trend in the main series for the mass loss, but with different values and classifications. At the lower wind speed of 3 m/s, the mass loss was the lowest compared to higher wind speeds and was classified as intermediate crowning, as it exceeded 65 %. With increasing wind speed, the mass loss became higher, reaching over 80 %, classifying it as sustained crowning.

For cases with a CBH of 10 m, no sustained crowning was observed, which aligns with Guo's observation [40] regarding the low probability of crowning at higher CBH levels. However, as the wind speed increased, the crown mass loss increased, suggesting a rising probability of crowning. Further increasing the wind speed from 8 m/s to 10 m/s (from case CBH10W8 to case CBH10W10) led to a slight rise in mass loss, suggesting a small increase in the likelihood of crowning. This indicates

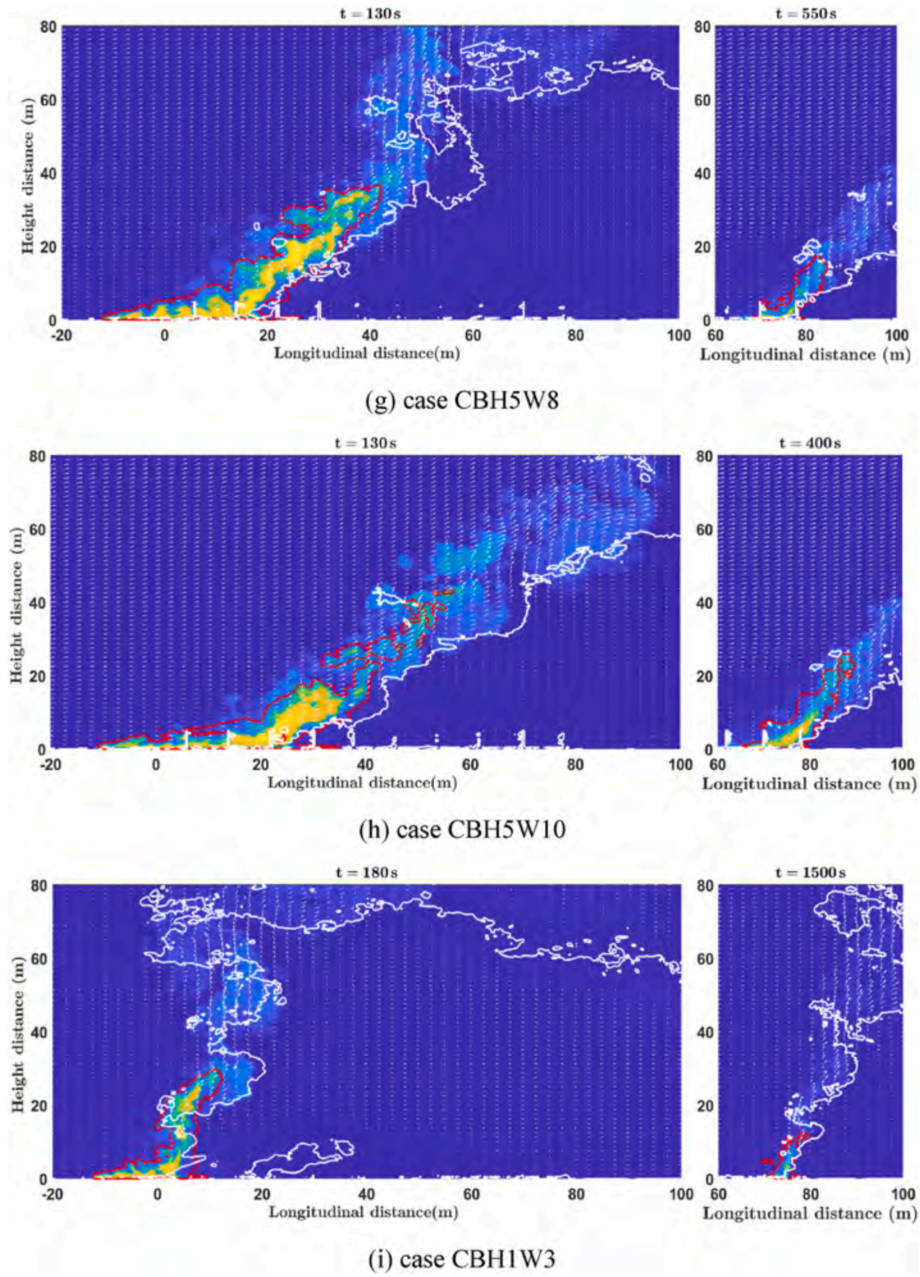

Fig. 8. (*continued*).

that beyond this wind speed, further increases may have little additional effect on the probability of crowning for this CBH. This pattern indicates that at this CBH, lower wind speeds prevent crowning, while very high wind speeds may push the surface fire to lower levels, reducing the likelihood of crown ignition. These findings align with observations from Scott [8].

3.6. Comparing the simulation results with the Cruz model

In this section, we will compare our simulation results with one of the most prominent empirical models created by Cruz et al. [20], which predicts the likelihood of crowning in pine plantations. According to the Cruz model, the crowning probability is determined by the CAC (Criteria for Active Crowning), which serves as a key indicator of whether a fire will result in active or passive crowning. The model is:

$$\text{CAC} = \frac{11.02 * {U_{10}}^{0.9} * CBD^{0.19} * e^{(-0.17EFFM)}}{3/CBD} \tag{4}$$

Where.

- U_{10} is the wind speed (km/h),
- CBD is the crown bulk density (kg/m^3),
- EFFM is the effective fuel moisture content (%).

The model interprets the CAC value as follows.

- If CAC >1, the fire will likely result in **active crowning.**
- If CAC <1, the fire will lead to **passive crowning.**

While CBH is not directly included in the CAC equation, its impact on fire transition is captured through CBD, which is influenced by crown

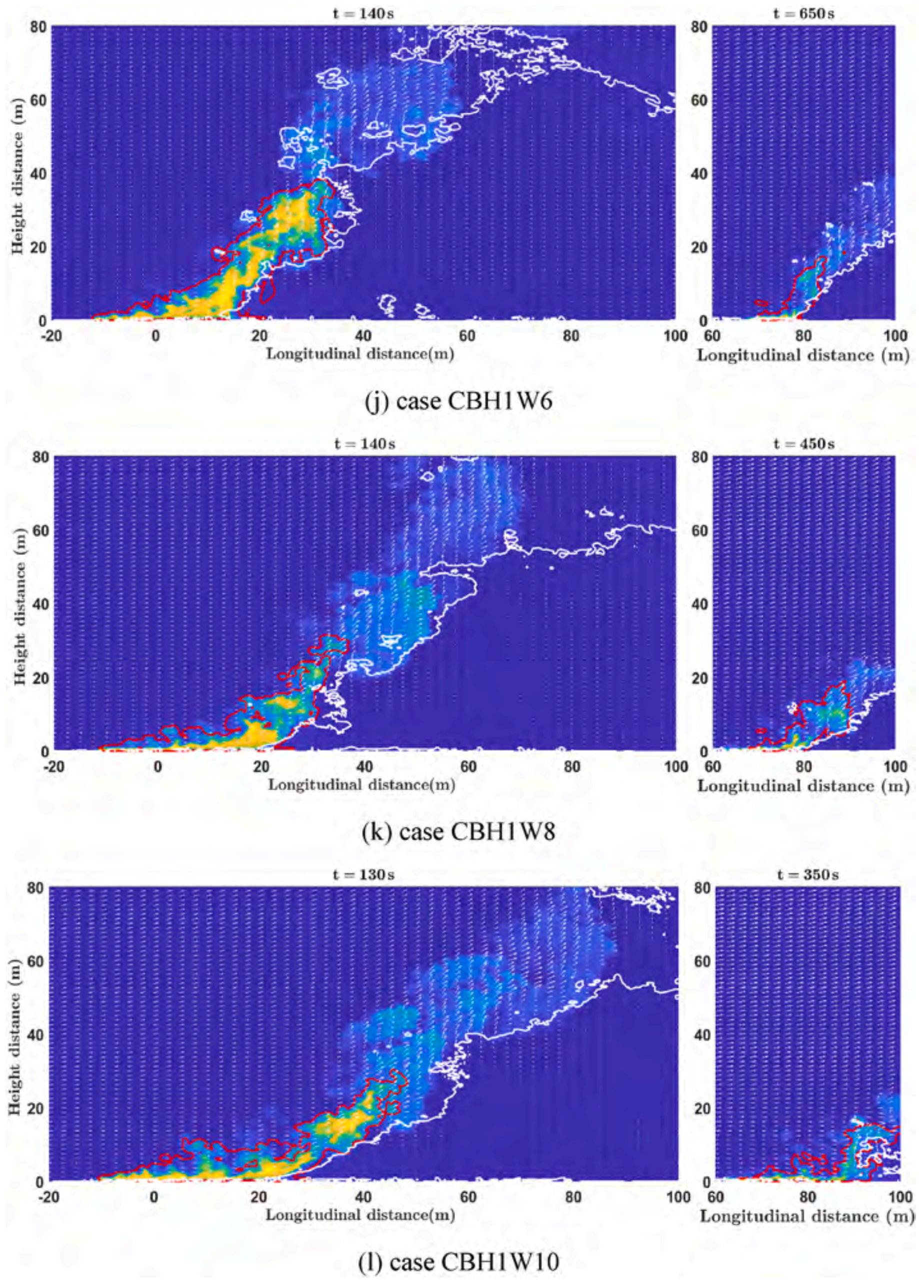

Fig. 8. (*continued*).

height (CH). As CH decreases, the crown's volume reduces, leading to an increase in CBD, given that the crown fuel load remains constant. Since CH and CBH are typically proportional—both increasing as the forest matures [28] —there is an inverse relationship between CBH and CBD. The CBD values for our cases with different CBH were calculated by dividing the crown fuel load (1 kg/m^2, as shown in Table 1) by the corresponding CH values.

From our simulation results, CBH is a critical factor in determining crowning potential. A lower CBH facilitates the transition of surface fire to the canopy, while a higher CBH acts as a barrier, reducing the likelihood of crown ignition; we can infer the effect of CBH on crowning by examining cases with the same wind speed but varying CBH values. For instance, comparing CAC values across cases with identical wind speeds but varying CBH values (e.g., CBH10W3, CBH5W3, and CBH1W3) demonstrates that the only parameter influencing the CAC calculation in these sets is CBD. Similar trends are observed for cases with higher wind speeds. We observe an inverse relationship between CAC values and CBH across all sets with the same wind speed. As CBH decreases, CBD increases, which in turn raises the CAC value, indicating a higher likelihood of crowning. This inverse relationship between CBH and CAC aligns with our simulation results, where reducing CBH increases the potential for sustained crowning.

Table 5 presents the calculated CAC values for each simulation case. In our analysis, cases with 80 % or more crown mass loss were classified as sustained crowning, while those with 65 %–80 % were categorized as intermediate crowning. Comparing these classifications with the crowning probabilities predicted by the Cruz model, we found that 9 out of 12 cases in the main simulation series aligned with the model's predictions. This alignment was reduced to 8 out of 12 in the modified series. Moreover, the CAC values derived from the Cruz model matched our classification criteria for crowning (both sustained and intermediate) and non-sustained crowning. These findings highlight a good correlation between the model's predictions and our simulation outcomes.

However, some discrepancies remain (e.g., in CBH10W8). These

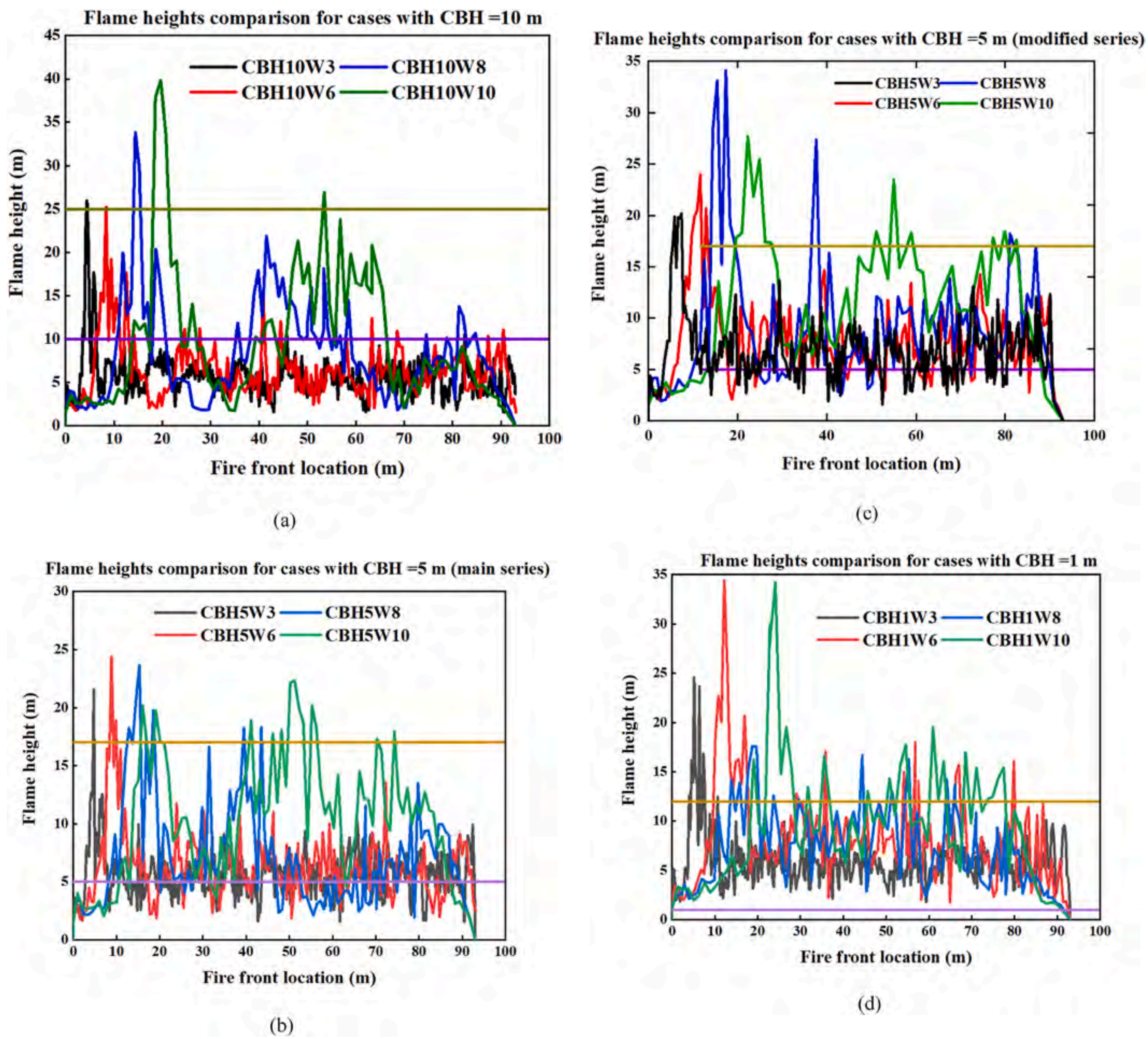

Fig. 9. Flame height comparisons for cases with (a) CBH = 10 m, (b) CBH = 5 m (main series), (C) CBH = 5 m (modified series), and (D) CBH = 1 m. Horizontal lines in each subplot mark the top of the crown (upper line) and the bottom edge (lower line) .

Table 3
The percentage of time when flame height is below, inside, and above the crown vegetation for each simulated case.

CBH10W3	0.29 % 2.61 % 97.1 %	CBH10W6	0.42 % 7.65 % 91.93 %	CBH10W8	1.3 % 32.25 % 66.45 %	CBH10W10	3.9 % 35.65 % 60.45 %
CBH5W3 (main series)	**0.3 %** **61.7 %** **38 %**	**CBH5W6 (main series)**	**0.84 %** **70.88 %** **28.28 %**	**CBH5W8 (main series)**	**4.16 %** **56.54 %** **39.3 %**	**CBH5W10 (main series)**	**16.12 %** **62.36 %** **21.52 %**
CBH5W3 (modified series)	**2.13 %** **71.36 %** **26.49 %**	**CBH5W6 (modified series)**	**3.47 %** **72.22 %** **24.31 %**	**CBH5W8 (modified series)**	**9.47 %** **65.26 %** **25.26 %**	**CBH5W10 (modified series)**	**18.84 %** **63.77 %** **17.39 %**
CBH1W3	**3.23 %** **96.77 %** **0 %**	**CBH1W6**	**13.73 %** **86.27 %** **0 %**	**CBH1W8**	**11.86 %** **88.14 %** **0 %**	**CBH1W10**	**28.12 %** **71.88 %** **0 %**

arise because the Cruz model does not incorporate CBH. For this reason, we used the Cruz model as a general indicator of transition potential rather than a precise predictor. While factors such as turbulence or potential overestimation of convective heating in FDS may also contribute to differences, the omission of CBH in the Cruz model is a primary limitation in explaining these inconsistencies.

Table 4
The percentage of flame height time inside the above and lower portions of the crown vegetation for each simulated case.

CBH10W3	0.87 %	CBH10W6	0.85 %	CBH10W8	4.51 %	CBH10W10	13.95 %
	1.74 %		6.8 %		27.74 %		21.7 %
CBH5W3 (main series)	**1.46 %**	**CBH5W6 (main series)**	**4.64 %**	**CBH5W8 (main series)**	**8.92 %**	**CBH5W10 (main series)**	**29.03 %**
	60.23 %		**66.24 %**		**47.61 %**		**33.33 %**
CBH5W3 (modified series)	**4.7 %**	**CBH5W6 (modified series)**	**15.27 %**	**CBH5W8 (modified series)**	**18.94 %**	**CBH5W10 (modified series)**	**31.88 %**
	66.66 %		**56.94 %**		**46.31 %**		**31.88 %**
CBH1W3	**28.15 %**	**CBH1W6**	**46.70 %**	**CBH1W8**	**39.83 %**	**CBH1W10**	**39.58 %**
	68.6 %		**39.56 %**		**48.3 %**		**32.29 %**

Table 5
Calculation of Crown Active Criteria (CAC) for our cases based on the Cruz equation. The shaded cells in the CAC and crown mass loss columns indicate cases where the crown fire predictions from the Cruz model align with our simulation results.

	wind speed m/s	wind speed km/hr	CBD Kg/m^3	EFFM %	CAC	Crown mass loss %
CBH10W3	3.00	10.80	0.07	5.00	0.53	30.8%
CBH10W6	6.00	21.60	0.07	5.00	0.99	47.7%
CBH10W8	8.00	28.80	0.07	5.00	1.29	51%
CBH10W10	10.00	36.00	0.07	5.00	1.57	47.90%
CBH5W3	3.00	10.80	0.08	5.00	0.69	78.06%
CBH5W6	6.00	21.60	0.08	5.00	1.30	84.29%
CBH5W8	8.00	28.80	0.08	5.00	1.68	83.67%
CBH5W10	10.00	36.00	0.08	5.00	2.05	82.59%
CBH1W3	3.00	10.80	0.09	5.00	0.77	97.85%
CBH1W6	6.00	21.60	0.09	5.00	1.44	99.05%
CBH1W8	8.00	28.80	0.09	5.00	1.86	98.82%
CBH1W10	10.00	36.00	0.09	5.00	2.28	98.67%

4. Conclusion

This study highlights the influence of crown base height (CBH) and wind speed on the transition of surface fires to crown fires under conditions of fixed moisture content. Our simulations, with a validated physics-based model, reveal that 80 % of crown mass loss dictates the likelihood of a sustained crown fire, while values between 65 % and 80 % correspond to intermediate crowning. A lower CBH increases the probability of transitioning to a crown fire, indicating a greater risk of crowning. The influence of wind speed on crown fire likelihood varies with CBH levels. For lower CBH values, wind speed exerts minimal impact on crown fire likelihood, as low CBH alone is sufficient to sustain crown fire initiation regardless of wind speed. However, for higher CBH values, crown fire probability is minimal at low wind speeds but increases with wind speeds. At very high wind speeds, the likelihood of crowning stabilizes. This occurs because the flames become highly elongated in the direction of the wind, causing the majority of heat transfer to be horizontal rather than vertical, which limits the heat available to ignite the crown. Additionally, the influence of species-specific thermo-physical properties on fire behaviour was examined through a modified simulation series.

The streamline analysis highlights the critical role of wind-driven flow patterns in shaping fire dynamics. As wind speed increases, the expansion of the flame-impacted crown vegetation area suggests a greater likelihood of sustained crowning, reinforcing the importance of wind speed in fire transition. The flame height assessment reinforces its role as a critical factor in fire transition, with higher flames leading to increased crown penetration and sustained fire spread. Cases with lower CBH and modified thermo-physical properties exhibit greater flame heights, resulting in prolonged crown involvement and higher crown mass loss.

By comparing our simulation results for sustain crowning (whether complete or intermediate) and non-sustain crowning cases with the Cruz empirical model, which predicts crowning in pine plantations, we found that 9 out of 12 cases in the main simulation series have the same predictions with the model. In the modified series, 8 out of 12 cases show the same agreement. Our simulations align with the model's equation, showing that for any given wind speed, a decrease in CBH increases the likelihood of crown fire initiation.

While this study provides valuable insights, the results are constrained by limitations such as the chosen numerical geometry, the simplified forest configuration, the absence of ladder fuels and ember transport, and the use of a fixed moisture content. Future research will focus on conducting simulations with varying moisture content levels to identify the threshold at which moisture content significantly influences crown fire potential. Simulations with varying surface fuel loads and different crown fuel loads will also be performed to assess their respective impacts on crown fire transition and initiation likelihood.

To enhance fire prevention in forest management, our findings suggest implementing strategic measures targeting CBH and wind dynamics. Raising CBH through selective pruning or thinning can significantly reduce the likelihood of surface fires transitioning to crown fires, particularly in areas with lower wind speeds. In high-wind regions, creating windbreaks or buffer zones with less flammable species can mitigate horizontal flame spread and limit crown fire initiation. Additionally, incorporating species with thermo-physical properties less conducive to ignition, such as those with higher moisture retention, can further reduce fire risk. These engineering interventions, informed by our simulation results, provide actionable strategies for designing fire-resilient forest ecosystems.

CRediT authorship contribution statement

Mohamed Sharaf: Writing – original draft, Methodology. **Duncan Sutherland:** Supervision. **Rahul Wadhwani:** Supervision. **Khalid Moinuddin:** Writing – review & editing, Supervision.

Declaration of competing interest

The authors declare the following financial interests/personal relationships which may be considered as potential competing interestsMOHAMED SHARAF reports financial support was provided by Victoria University. MOHAMED SHARAF reports a relationship with Natural Hazards Research Australia that includes: funding grants. This research was conducted with the assistance of computational resources provided by the National Computational Infrastructure (NCI Australia), an NCRIS-enabled capability supported by theAustralian Government. If there are other authors, they declare that they have no known competing financial interests or personal relationships that could have appeared to influence the work reported in this paper.

Acknowledge

This research was supported by funding from Natural Hazards Research Australia NHRA, whose support made this project possible. I am grateful to **Dr. Nazmul Khan** for his invaluable guidance and support throughout the research process. His expertise and encouragement were instrumental in the completion of this study. Additionally, this research was conducted with the assistance of computational resources provided by the National Computational Infrastructure (NCI Australia), an NCRIS-enabled capability supported by theAustralian Government.

Appendix A. Sensitivity analysis

In this section, we present the sensitivity analysis for the remaining parameters, including domain height, the distance between the ignition line and the inlet, the distance from the end of the burnable plot to the outlet, and the intensity of the ignition line.

A.1 Domain height

We simulated scenarios with domain heights of 60 m, 80 m, and 100 m, using a grid size of 0.25 m, to assess their impact on HRR and MLR. The results show minimal differences in HRR (Figure A.1a) and MLR (Figure A.1b) between 80 m and 100 m, while the 60 m case exhibits noticeable variations. A domain height of 80 m is sufficient for accurate simulations, as the 60 m height, being only 2.4 times the tallest forest height (25 m), is inadequate for capturing detailed flame dynamics.

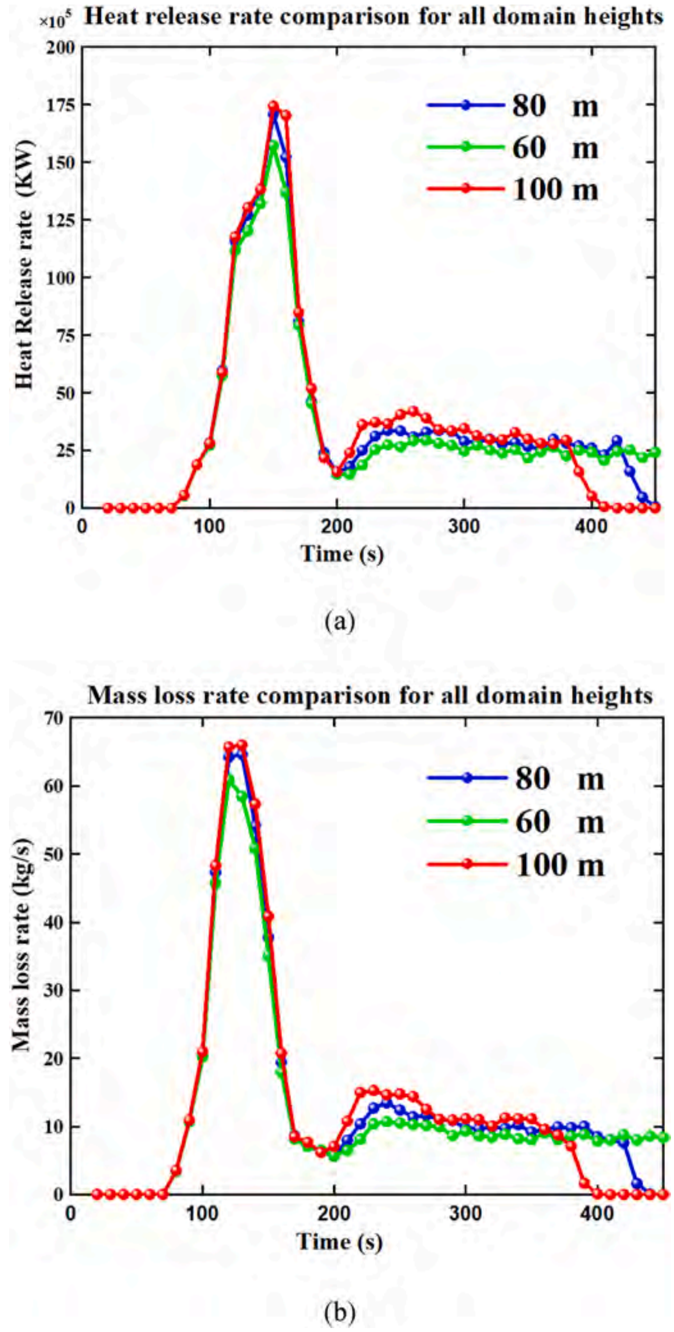

Fig. A.1. (a) Comparison of HRR and (b) MLR for three cases with different domain heights.

A.2 Distance of ignition line from inlet

In this section, we conducted simulations using three different distances for the ignition line from the inlet: 85 m, 105 m, and 125 m to see the effect of boundary layer development on fire growth. The results, depicted in Figure A.2, allow us to compare the outcomes for HRR and MLR across these cases. As shown in Figures A.2(a) and A.2(b), the HRR and MLR exhibit no noticeable differences between the distances of 105 m and 125 m. This suggests that using 105 m, the boundary layer is well developed.

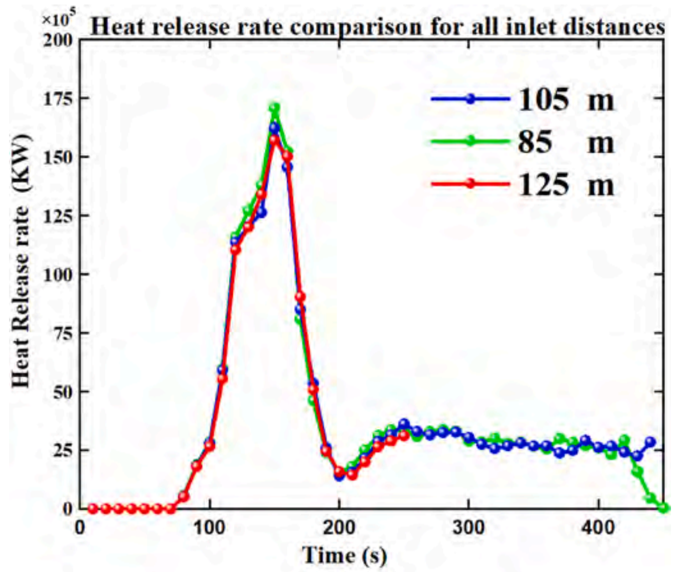

(a)

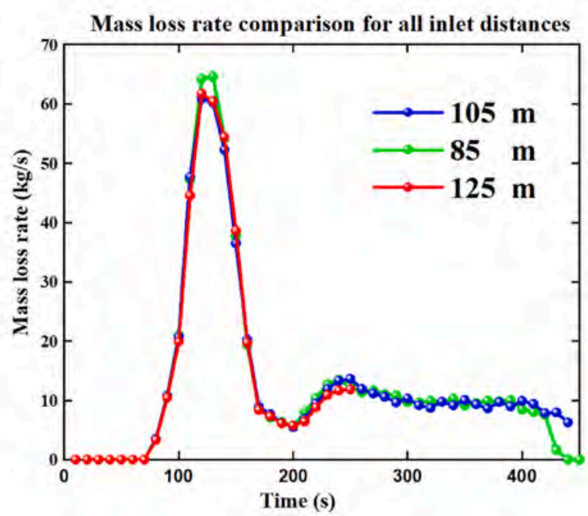

(b)

Fig. A.2. (a) Comparison of HRR and (b) MLR for three cases with different distances for the ignition line from the inlet.

To verify the well-developed flow in our domain from these cases, we plotted wind velocity profiles at various x-locations, ranging from the inlet to the point at x = 0 (the start of the vegetation), along the geometric centreline (y = 0), as shown in Figure A.3. The velocities presented are time-averaged values along the centreline of the domain derived from the u-velocity slice files processed using MATLAB. These figures indicate minimal variations in velocities, demonstrating that stable wind fields are established in all cases. This also suggests that an inlet distance of 105 m can be used in our simulations.

The x-axis in these plots represents the ratio between the wind speed variation across the domain height and the actual wind speed at a height of 10 m, denoted as U_{10}. The x-position of −15 m was selected as the reference point for U_{10} since it corresponds to the location of the fire line. This reference point ensures consistency in evaluating wind speed variations. Another critical factor in determining the distance of the ignition line from the inlet is the variation in U_{10}. The U_{10}values at distances of 85 m, 105 m, and 125 m are 6.93 m/s, 6.71 m/s, and 6.66 m/s, respectively. The difference between the values at 85 m and 105 m is 3.1 %, while the difference between 105 m and 125 m is only 0.7 %. This indicates that increasing the inlet distance beyond 105 m has a negligible impact on U_{10}, suggesting 105 m is a reasonable inlet distance for stabilizing the wind speed.

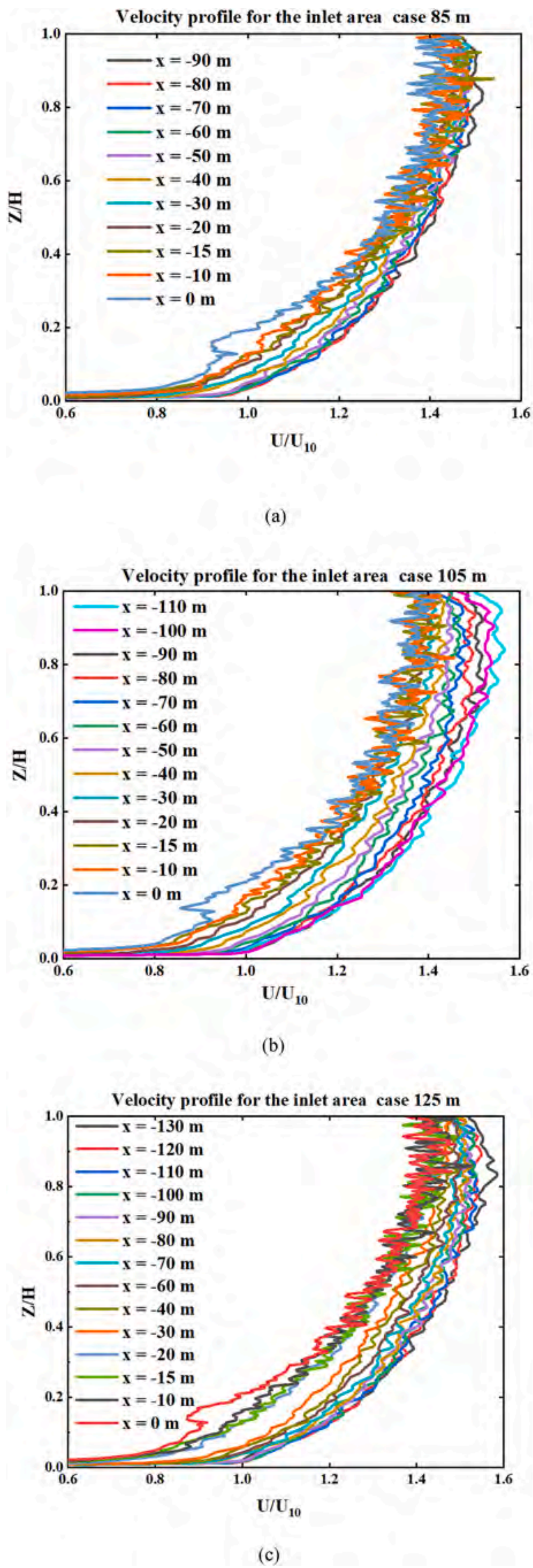

Fig. A.3. Velocity profile for the inlet area across three cases: (a) Case 85 m, (b) Case 105 m, and (c) Case 125 m.

A.3 Distance from the end of the burnable plot to the outlet

In this section, we analysed three different distances between the end of the burnable plot and the outlet: 40 m, 60 m, and 80 m. The results of HRR and MLR are illustrated in Figure A.4, which reveals that these two outputs remain almost consistent between the 60 m and 80 m distances. This indicates that increasing the distance beyond 60 m does not significantly alter the outcomes, making 60 m the more efficient choice in terms of computational resources.

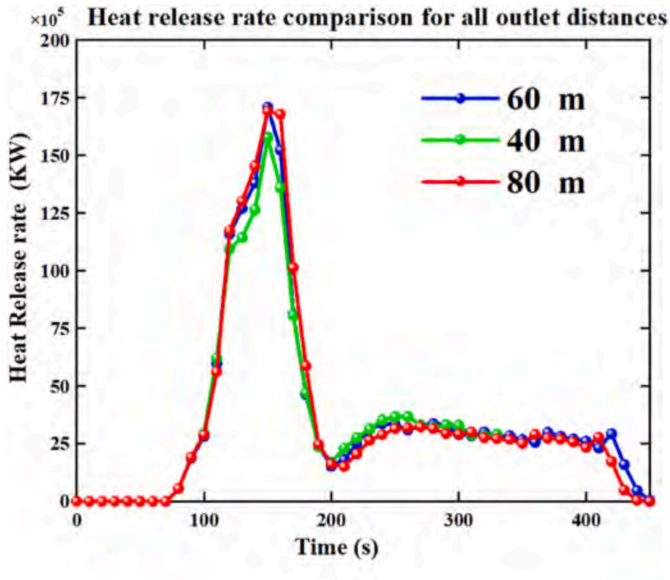

(a)

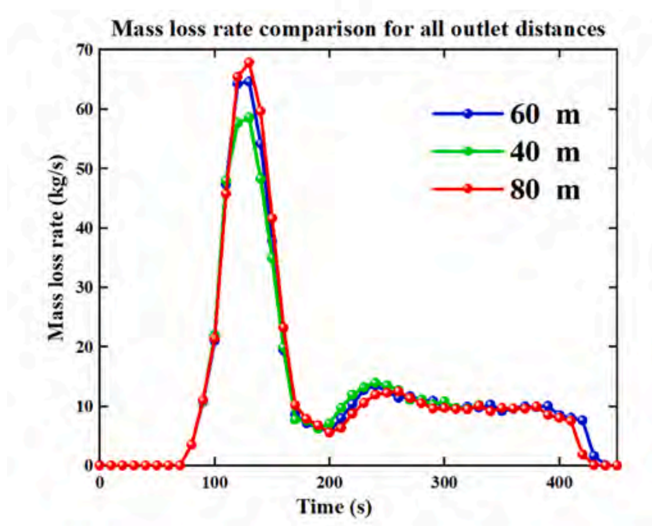

(b)

Fig. A.4. (a) Comparison of HRR and (b) MLR for three cases with different distances between the end of the burnable plot and the outlet.

A.4 Ignition line intensity (HRRPUA)

In this section, we conducted simulations for three different ignition line intensities (HRRPUA): 1000 kW/m^2, 2000 kW/m^2, and 3000 kW/m^2. The results are presented in Figure A.5. As depicted in Figures A.5 (a) and A.5 (b), there is no noticeable difference in the HRR and MLR between the HRRPUA values of 1000 kW/m^2, 2000 kW/m^2, and 3000 kW/m^2, so all of them are roughly consistent. However, the 1000 kW/m^2 case shows a slight difference in both HRR and MLR compared to the other two values. HRRPUA of 2000 kW/m^2 is chosen for our simulations.

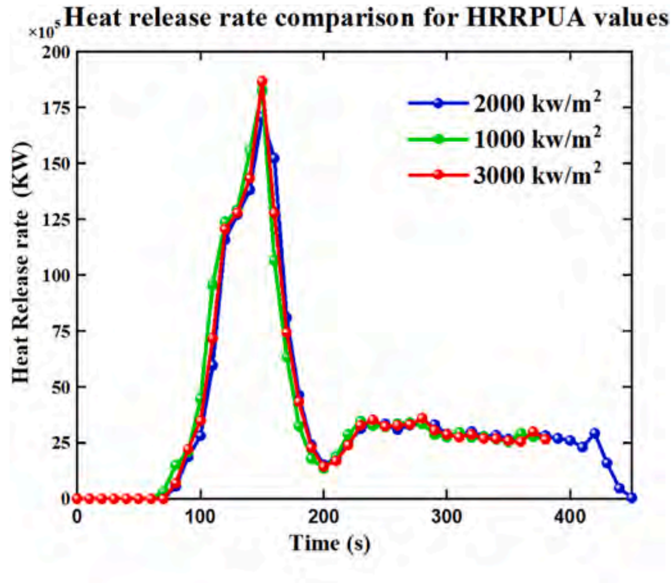

(a)

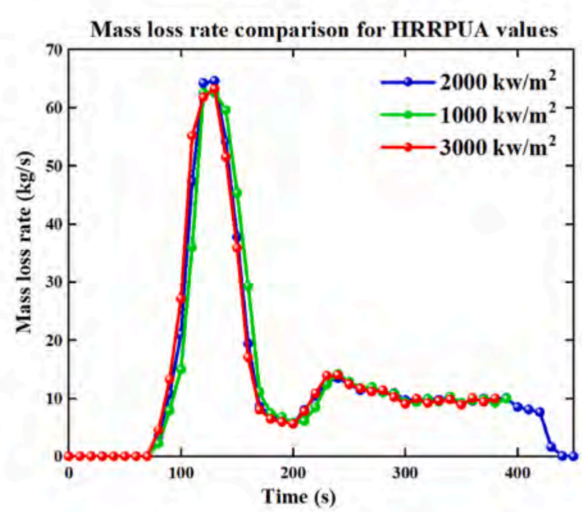

(b)

Fig. A.5. (a) Comparison of HRR and (b) MLR for three cases with different HRRPUA values.

The final selected values for this study are summarised in Table A.1.

Table A.1
The final parameter was obtained from the sensitive analysis study.

No	parameter	unit	value	Figure
1	Grid size	m	0.25	Fig. 2
2	Domain height	m	80	Figure A.1
3	Distance of the ignition line from the inlet	m	105	Figures A.2+A.3
4	Distance from the end of the burnable plot to the outlet	m	60	Figure A.4
5	HRRPUA	kW/m^2	2000	Figure A.5

Appendix B. Summary of results for the modified simulation series

Figure B.1 presents the crown mass loss for all simulated cases in the modified series and shows a trend similar to that observed in Fig. 3 for the main series. For cases with a fixed crown base height (CBH), increasing wind speed leads to a higher crown mass loss rate. However, the mass loss in this modified series is generally higher than in the main series. The case with the lowest wind speed and highest CBH exhibits minimal crown mass loss, indicating the absence of crown fire, while the case with the lowest CBH and highest wind speed shows nearly complete crown consumption, indicating sustained crown fire.

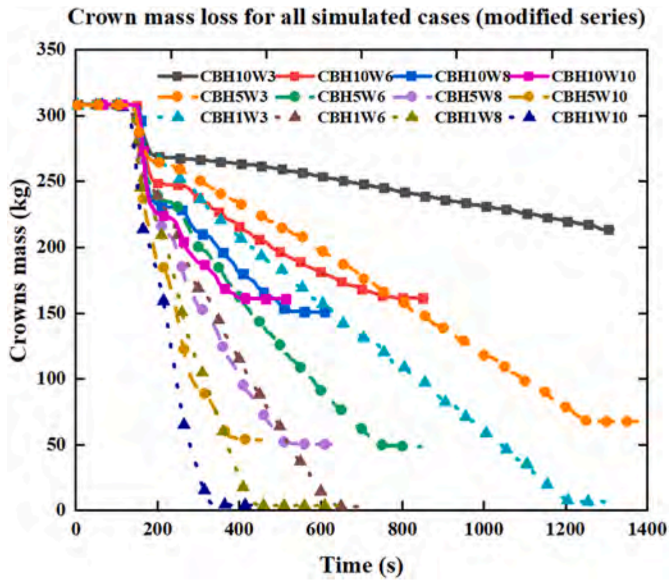

Fig. B.1. Crown mass loss for all cases in the modified series. The figure follows the same structure as Fig. 4.

Figure B.2 presents both the percentage of crown mass loss and the duration of crown consumption for each case in the modified series. Across all cases, the mass loss is consistently higher than in the main series, while the time taken for crown consumption is generally shorter. Cases with lower CBH experience nearly complete crown consumption, indicating crown fire, while intermediate CBH cases show substantial but comparatively lower crown mass loss. In contrast, the case with the highest CBH exhibits the lowest crown mass loss, suggesting a very low likelihood of crown fire. Additionally, increasing wind speed leads to shorter crown mass loss durations.

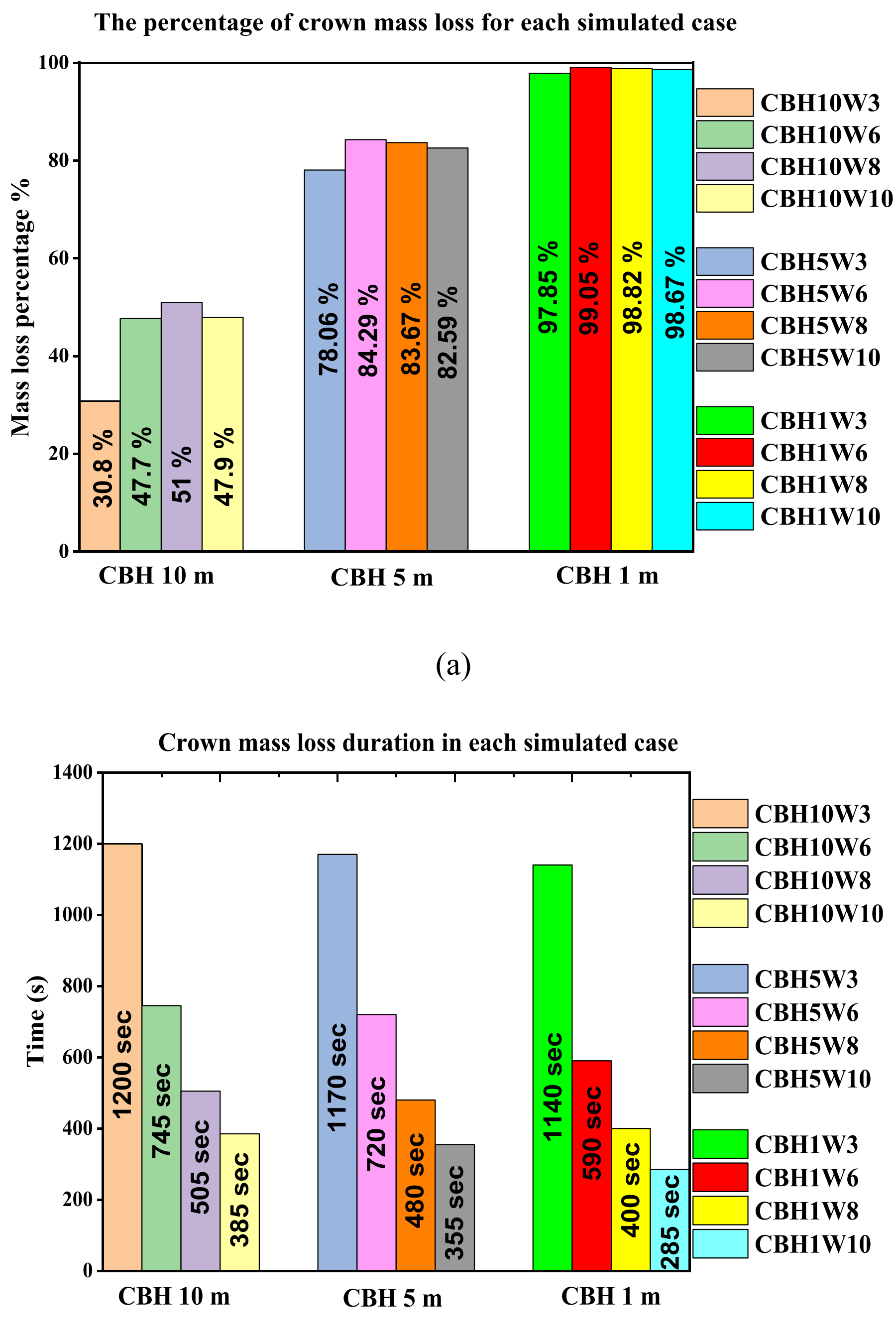

Fig. B.2. (a) Crown mass loss percentage and (b) crown mass loss duration for each case in the modified series.

Table B.1 compares the Crown Active Criteria (CAC) values—used to assess crowning probability in the Cruz model—with the calculated crown mass loss from our modified series of simulations. We classify cases with crown mass loss above 80 % as sustained crowning and those between 65 % and 80 % as intermediate crowning. Based on this classification, 8 out of 12 cases show agreement between the Cruz model predictions and our simulation results. Cases with matching outcomes are highlighted in the CAC and crown mass loss columns.

Table B.1
Comparison of CAC values from the Cruz model and crown mass loss from simulations (modified series). Shaded cells indicate agreement between the two methods.

	wind speed m/s	wind speed km/hr	CBD Kg/m^3	EFFM %	CAC	Crown mass loss %
CBH10W3	**3.00**	**10.80**	**0.07**	**5.00**	**0.53**	**30.8 %**
CBH10W6	**6.00**	**21.60**	**0.07**	**5.00**	**0.99**	**47.7 %**

(continued on next page)

Table B.1 (*continued*)

	wind speed m/s	wind speed km/hr	CBD Kg/m^3	EFFM %	CAC	Crown mass loss %
CBH10W8	**8.00**	**28.80**	**0.07**	**5.00**	**1.29**	**51 %**
CBH10W10	**10.00**	**36.00**	**0.07**	**5.00**	**1.57**	**47.90 %**
CBH5W3	**3.00**	**10.80**	**0.08**	**5.00**	**0.69**	**78.06 %**
CBH5W6	**6.00**	**21.60**	**0.08**	**5.00**	**1.30**	**84.29 %**
CBH5W8	**8.00**	**28.80**	**0.08**	**5.00**	**1.68**	**83.67 %**
CBH5W10	**10.00**	**36.00**	**0.08**	**5.00**	**2.05**	**82.59 %**
CBH1W3	**3.00**	**10.80**	**0.09**	**5.00**	**0.77**	**97.85 %**
CBH1W6	**6.00**	**21.60**	**0.09**	**5.00**	**1.44**	**99.05 %**
CBH1W8	**8.00**	**28.80**	**0.09**	**5.00**	**1.86**	**98.82 %**
CBH1W10	**10.00**	**36.00**	**0.09**	**5.00**	**2.28**	**98.67 %**

Data availability

Data will be made available on request.

References

[1] M. Bennett, et al., Reducing Fire Risk on Your Forest Property, 2010.
[2] D.X. Viegas, L. Ribeiro, M. Viegas, L. Pita, C. Rossa, Impacts of fire on society: extreme fire propagation issues, Earth observation of wildland fires in Mediterranean ecosystems (2009) 97–109.
[3] C.V. Wagner, Conditions for the start and spread of crown fire, Can. J. For. Res. 7 (1) (1977) 23–34.
[4] J. Beck, et al., Fire ecology and management, in: Forestry Handbook for British Columbia, fifth ed., Forestry Undergraduate Society, Faculty of Forestry, UBC. Vancouver, BC, 2005, pp. 490–525.
[5] F. Hines, F. Hines, K.G. Tolhurst, A.A. Wilson, G.J. McCarthy, Overall Fuel Hazard Assessment Guide, Victorian Government, Department of Sustainability and Environment East …, 2010.
[6] J.K. Agee, C.N. Skinner, Basic principles of forest fuel reduction treatments, For. Ecol. Manag. 211 (1–2) (2005) 83–96.
[7] R.R. Linn, P. Cunningham, Numerical simulations of grass fires using a coupled atmosphere–fire model: basic fire behavior and dependence on wind speed, J. Geophys. Res. Atmos. 110 (D13) (2005).
[8] J.H. Scott, *Comparison of Crown Fire Modeling Systems Used in Three Fire Management Applications* (No. 58), US Department of Agriculture, Forest Service, Rocky Mountain Research Station, 1998.
[9] J.S. Clark, Particle motion and the theory of charcoal analysis: source area, transport, deposition, and sampling, Quat. Res. 30 (1) (1988) 67–80.
[10] A. Grishin, V. Perminov, Transition of the forest ground fire to crown fire, Combust. Explos. Shock Waves 26 (6) (1990) 644–651.
[11] J.H. Scott, *Assessing crown Fire Potential by Linking Models of Surface and Crown Fire Behavior* (No. 29), US Department of Agriculture, Forest Service, Rocky Mountain Research Station, 2001.
[12] M. Gomes da Cruz, Modeling the Initiation and Spread of Crown Fires, 1999.
[13] M.G. Cruz, M.E. Alexander, R.H. Wakimoto, Predicting crown fire behavior to support forest fire management decision-making, in: IV International Conference on Forest Fire Research, vol. 11, 2002. DX Viegas.
[14] M.G. Cruz, M.E. Alexander, R.H. Wakimoto, Assessing canopy fuel stratum characteristics in crown fire prone fuel types of western North America, Int. J. Wildland Fire 12 (1) (2003) 39–50.
[15] M.G. Cruz, M.E. Alexander, R.H. Wakimoto, Assessing the probability of crown fire initiation based on fire danger indices, For. Chron. 79 (5) (2003) 976–983.
[16] M.G. Cruz, M.E. Alexander, R.H. Wakimoto, Modeling the likelihood of crown fire occurrence in conifer forest stands, For. Sci. 50 (5) (2004) 640–658.
[17] M.G. Cruz, M.E. Alexander, R.H. Wakimoto, Development and testing of models for predicting crown fire rate of spread in conifer forest stands, Can. J. For. Res. 35 (7) (2005) 1626–1639.
[18] M.G. Cruz, B.W. Butler, M.E. Alexander, J.M. Forthofer, R.H. Wakimoto, Predicting the ignition of crown fuels above a spreading surface fire. Part I: model idealization, Int. J. Wildland Fire 15 (1) (2006) 47–60.
[19] M.G. Cruz, B.W. Butler, M.E. Alexander, Predicting the ignition of crown fuels above a spreading surface fire. Part II: model evaluation, Int. J. Wildland Fire 15 (1) (2006) 61–72.
[20] M.E. Alexander, M.G. Cruz, Evaluating a model for predicting active crown fire rate of spread using wildfire observations, Can. J. For. Res. 36 (11) (2006) 3015–3028, https://doi.org/10.1139/x06-174.
[21] T. Beer, The interaction of wind and fire, Boundary-Layer Meteorol. 54 (3) (1991) 287–308.
[22] E.V. Mueller, Z. Campbell-Lochrie, C. Walker-Ravena, R.M. Hadden, Numerical simulations of flame spread in pine needle beds using simple thermal decomposition models, Fire Saf. J. 141 (2023), https://doi.org/10.1016/j.firesaf.2023.103886.
[23] R. Wadhwani, D. Sutherland, K. Moinuddin, X. Huang, Numerical simulation of two parallel merging wildfires, Int. J. Wildland Fire 32 (12) (2023) 1726–1740, https://doi.org/10.1071/wf23071.
[24] S. Gupta, M. Sharaf, M. Arun, M. Guerrierri, K. Moinuddin, Experimental and numerical investigation of burning characteristics of Australian pine trees for wildfire modelling, Fire Saf. J. (2025/08/17/2025) 104500, https://doi.org/10.1016/j.firesaf.2025.104500.
[25] D. Castle, W.E. Mell, F.J. Miller, Examination of the Wildland-urban interface Fire Dynamics Simulator in modeling of laboratory-scale surface-to-crown fire transition, in: Proceedings of the 8th US National Combustion Meeting, vol. 4, 2013, pp. 3710–3722. Park City, UT, USA.
[26] K.A.M. Moinuddin, D. Sutherland, Modelling of tree fires and fires transitioning from the forest floor to the canopy with a physics-based model, Math. Comput. Simulat. 175 (2020) 81–95, https://doi.org/10.1016/j.matcom.2019.05.018.
[27] K. McGrattan, Fire Dynamics Simulator User's Guide, vol. 6, NIST special publication1019, 2013.
[28] M. Cruz, P. de Mar, D. Adshead, Radiata Pine Plantation Fuel and Fire Behaviour Guide, GHD, 2011. www.ghd.com/PDF/PinusRadiataFuelandFireGuide.pdf [Verified 4 April 2017].
[29] E. Bou-Zeid, J. Overney, B.D. Rogers, M.B. Parlange, The effects of building representation and Clustering in large-Eddy simulations of flows in urban canopies, Boundary-Layer Meteorol. 132 (3) (2009) 415–436, https://doi.org/10.1007/s10546-009-9410-6.
[30] M. Yurtgan, I. Baysal, O. Küçük, Fuel characterization and crown fuel load prediction in non-treated Calabrian pine (Pinus brutia Ten.) plantation areas, iFor. Biogeosci. For. 15 (6) (2022) 458–464, https://doi.org/10.3832/ifor4048-015.
[31] N. Çepel, O.Y.M.Ö. Tekerek, Antalya Orman Bölge Basmüdürlügü yöresinde bazi saf kizilçam mescerelerinin ölü örtü miktari üzerine arastirmalar [Investigations on the amount of litter of some pure Calabrian pine stands in Antalya Regional Directorate of Forestry], Journal of the Faculty of Forestry, Istanbul University 30 (1) (2012) 111–128.
[32] M.G. Cruz, J.S. Gould, M.E. Alexander, A.L. Sullivan, W.L. McCaw, S. Matthews, A Guide to Rate of Fire Spread Models for Australian Vegetation, Australasian Fire and Emergency Service Authorities Council Limited and …, 2015.
[33] I. Noble, A. Gill, G. Bary, McArthur's fire-danger meters expressed as equations, Aust. J. Ecol. 5 (2) (1980) 201–203.
[34] K.B. McGrattan, Techinical Reference Guide, 2006, https://doi.org/10.6028/nist.Sp.1018.
[35] R. Wadhwani, Physics-based Simulation of Short-Range Spotting in Wildfires, Victoria University, 2019.
[36] D. Morvan, Physical phenomena and length scales governing the behaviour of wildfires: a case for physical modelling, Fire Technol. 47 (2) (2010) 437–460, https://doi.org/10.1007/s10694-010-0160-2.
[37] E. Eftekharian, M. Ghodrat, Y. He, R.H. Ong, K.C. Kwok, M. Zhao, Numerical analysis of wind velocity effects on fire-wind enhancement, Int. J. Heat Fluid Flow 80 (2019) 108471.
[38] E. Eftekharian, M. Ghodrat, Y. He, R.H. Ong, K.C. Kwok, M. Zhao, Correlations for fire-wind enhancement flow characteristics based on LES simulations, Int. J. Heat Fluid Flow 82 (2020) 108558.
[39] J. Cobian-Iñiguez, A. Aminfar, D.R. Weise, M. Princevac, On the use of semi-empirical flame models for spreading chaparral crown fire, Front. Mech. Eng. 5 (2019) 50, https://doi.org/10.3389/fmech.2019.00050.
[40] H. Guo, et al., Transition from Surface Fire to Crown Fire and Effects of Crown Height, Moisture Content and Tree Flower, Fire Technology, 2022, https://doi.org/10.1007/s10694-022-01262-x.